NASA CONTRACTOR REPORT

NASA CR-1936

A FINITE ELEMENT PROCEDURE FOR NONLINEAR PREBUCKLING AND INITIAL POSTBUCKLING ANALYSIS

by S.-T. Mau and R. H. Gallagher

Prepared by
CORNELL UNIVERSITY
Ithaca, N.Y. 14850
for Langley Research Center

NATIONAL AERONAUTICS AND SPACE ADMINISTRATION • WASHINGTON, D. C. • JANUARY 1972

1. Report No.	2. Government Accession No.	3. Recipient's Catalog No.
NASA CR-1936		

4. Title and Subtitle
A FINITE ELEMENT PROCEDURE FOR NONLINEAR PREBUCKLING AND INITIAL POSTBUCKLING ANALYSIS

5. Report Date
January 1972

6. Performing Organization Code

7. Author(s)
S.-T. Mau and R. H. Gallagher

8. Performing Organization Report No.

9. Performing Organization Name and Address
Cornell University
Ithaca, New York

10. Work Unit No.
126-14-16-01

11. Contract or Grant No.
NGR 33-010-070

12. Sponsoring Agency Name and Address
National Aeronautics and Space Administration
Washington, D.C. 20546

13. Type of Report and Period Covered
Contractor Report

14. Sponsoring Agency Code

15. Supplementary Notes

16. Abstract

A procedure cast in a form appropriate to the finite element method is presented for geometrically nonlinear prebuckling and postbuckling structural analysis, including the identification of snap-through type of buckling. The principal features of this procedure are the use of direct iteration for solution of the nonlinear algebraic equations in the prebuckling range, an interpolation scheme for determination of the initial bifurcation point, a perturbation method in definition of the load-displacement behavior through the postbuckling regime, and extrapolation in determination of the limit point for snap-through buckling. Three numerical examples are presented in illustration of the procedure and in comparison with alternative approaches.

17. Key Words (Suggested by Author(s))	18. Distribution Statement
Finite element methods, buckling analysis, nonlinear analysis, imperfection sensitivity	Unclassified

19. Security Classif. (of this report)	20. Security Classif. (of this page)	21. No. of Pages	22. Price*
Unclassified	Unclassified	56	$3.00

*For sale by the National Technical Information Service, Springfield, Virginia 22151

TABLE OF CONTENTS

LIST OF SYMBOLS

A	Cross-sectional area of arch.
$b_o, b_1 \ldots b_m$	Coefficients in the extrapolation formula of λ and Det.
Det, Det_i	Determinant of the total stiffness matrix and Determinant at the ith load level.
$D_1, D_2, \ldots D_7$, D_{31}, D_{51}	Coefficients in the parametric formulas of load and displacement.
e_1, e_{11}, e_{111}	Derivatives of e w.r.t. the perturbation parameter.
EI	Flexural rigidity of the beam and arch cross-section.
$\{f_e\}, \{f_e'\}, \{f_e''\}$	Field function of lateral displacement of beam and its derivatives w.r.t. element coordinate ξ.
$\{F\}, F_i$	Element nodal force vector and component.
h	Depth of the cross-section of the circular arch and plate thickness.
$\{I\}, I_i$	Pattern of imperfection and component.
$[k]$, k_{ij}	Element linear stiffness matrix and coefficients.
$[K]$, K_{ij}	System linear stiffness matrix and coefficients.
k_1, k_2, k_3	Spring constants of the non-linear foundation.
$\bar{K}_{ij}, \bar{K}'_{ij}, \bar{K}''_{ij}$	Matrices associated with the pre-buckling solution.
ℓ	Length of an element of the beam.
L	Length of the beam.
M	Applied moment.
$[n_1(\Delta)], [n_2(\Delta^2)]$	Element geometric stiffness matrices.
$[N_1(\Delta)], (N_2(\Delta^2)]$, N_{ijk}, $N_{ijk\ell}$	Structure geometric stiffness matrices and coefficients.
$\bar{N}_{ijk}$, $\bar{N}'_{ijk}$	Coefficients associated with the prebuckling displacements and their derivatives respectively.
$[N]$	Aggregate geometric stiffness matrix
p_o	Arch uniform load intensity.

$\{P\}$, P_i	Structure nodal force vector and component.
R	Circular arch radius.
u,v,w	Displacement components.
w_o	Beam initial displacement.
γ	Imperfection parameter.
$\{\Delta\},\Delta_i$	Displacements.
$\{\bar{\Delta}\},\bar{\Delta}_i$	Prebuckling displacements.
$\{\Delta^p\},\Delta_i^p$	Additional post-buckling displacements.
$\{\bar{\Delta}^c\},\{\bar{\Delta}'^c\},\{\bar{\Delta}''^c\}$	Prebuckling displacement at bifurcation load and their derivatives.
$\{\Delta_1\}$ Δ_{i1},$\{\Delta_2\}$,Δ_{i2}	Components of the post-buckling displacements.
$\Delta_{i_{21}}$,$\Delta_{i_{22}}$	Components of Δ_{i_2}.
Δ_s	The displacement chosen to be the path parameter ε.
Δ_{S1},Δ_{S2},Δ_{S3}	Components of Δ_s^p in the power series expansion.
Δ_{ij}	Value of Δ_i at load level λ_j.
ε	Path parameter.
ε_θ	Axial strain of the arch.
θ,θ_o	Arch circumferential coordinate and total angle.
λ	Nondimensional load parameter.
λ_i	The ith load level.
λ^c,λ_u	Bifurcation load, limit load.
$\Gamma_1,\Gamma_2,\Gamma_3$	Coefficients in the perturbation equation.
ρ	Radial distance measured from the arch middle surface.
ϕ_1,ϕ_2	Nodal slopes of the beam element.
ξ	Element local coordinate.
Π_p,Π_{p_i}	Potential energy and ith component of potential energy (i=1,2,3).

I. INTRODUCTION

The analysis of instability phenomena of complicated thin shells has drawn intensified interest due, in part, to the development of finite element analysis procedures for such structures.[1] It is well known that structures of this class collapse at load levels which are less than those predicted by linear instability theory because of the role played by initial imperfections and geometric nonlinearities. The extensive efforts in the development of theories to cope with the latter considerations have been surveyed by Hutchinson and Koiter[2]. Other noteworthy surveys have been written by Haftka, et al[3] and Bienek[4].

Although the various types of instability phenomena which might occur in the complete range of load-displacement behavior prior to final collapse are not as yet fully understood, certain forms are known and are of considerable practical importance, especially those which occur in the earliest stages of loading. These are illustrated in Figure 1. Curve a applies to "perfect" structures and represents the case in which the structure first displaces along the path defined by OAB (the fundamental path) and bifurcates (or branches) at the Point A to another path, OC. In contrast to a rising postbuckling path, as OC, a descending path OD (as pictured in Figure 1b) may be encountered.

When the structure possesses fabricational imperfections the load-displacement behavior follows the paths indicated by dotted lines. The structure with a rising postbuckling path will have strength exceeding the bifurcation load. The strength of an imperfect structure with a descending postbuckling path in the perfect state will not achieve strengths as high as the bifurcation load. Such structures, under the appropriate load condition, are termed "imperfection sensitive" and the maximum load attained (Point E) is termed the "limit point".

A non-bifurcating load-displacement behavior may also occur for a structure assumed to be devoid of imperfections and may take the form shown in Figure 1c, which is similar in shape to the curve OE (Figure 1b) of the imperfection-sensitive structure. Thus, a limit point is again encountered, at G, and the buckling

phenomenon is of the 'snap-through' type.

A landmark development of procedures for establishing the shape of the postbuckling path and for determining the limit point for imperfection-sensitive structures is due to Koiter.[5] Using the concept of perturbations from the bifurcation point, this approach enables an efficient definition of load-displacement behavior in the immediate postbuckling range. Further contributions or alternative forms of these concepts, in the classical vein, have been presented by Budiansky and Hutchinson[6], Sewell[7], and Thompson[8,9].

Extensions of Koiter's procedure to the format of finite element analysis, as well as other finite element approaches to the same physical problem, have appeared[10-13]. Morin[10] applies a predictor-corrector scheme in calculation of non-linear prebuckling behavior, in which a perturbation approach is employed as the predictor and Newton-Raphson iteration is employed as the corrector. The perturbation approach, in both the pre- and post-buckling computational phases, draws heavily upon earlier work by Thompson and Walker[11]. Thompson has also advocated a new perturbation approach (Reference 9) for the subject type of problem. Haftka, et al[3] propose the definition of an "equivalent structure", one in which the nonlinear terms are treated as initial imperfections, in order to exploit the concepts derived by Koiter for imperfect structures. Dupuis, et al[12], attack the solution of the nonlinear equations in an incremental-iterative manner. The work by Lang[13] is a direct adaptation of Koiter's concepts, including retention of the condition of a linear prebuckling state.

Recent analyses for both idealized structures[14] and for thin shells[15] have shown that the assumption of a linear prebuckling state may lead to inaccurate results. One of the principal aspects of the work described in this report is the method of determination of the load, and displacement state on the fundamental path, at the bifurcation point following upon a nonlinear prebuckling state. The information so-calculated

furnishes the necessary ingredients for an analysis of the post-buckling or limit point behavior. Additionally, a new method for calculating the limit point of a perfect structure is suggested by the method of pre-buckling analysis.

The starting point of the present small strain-finite displacement formulation is the definition of element stiffness equations in the Lagrangian frame of reference. The element stiffness matrices extend to both first- and second-degree geometric nonlinearities in the element displacement parameters. Then, direct iteration is used for solution of the nonlinear algebraic equations in the prebuckling range. Unlike many widely used and seemingly computationally more efficient procedures, direct iteration permits calculation of the fundamental path beyond the bifurcation point. Definition of the latter is accomplished by interpolation of the determinants of such solutions through the zero point.

For postbuckling, and for snap-through buckling for initial-imperfection situations, both displacements and loads are expanded about the bifurcation point of the perfect structure in power series in a single parameter which is related to the amplitude of the eigen-function in the deflected shape of the structure. Upon determination of the series coefficients, the solution is a parametric representation of load vs. displacement.

As indicated above, a new procedure is devised for the case of the limit point analysis of perfect structures. This procedure, which requires little more than the calculation of the determinants of the system (nonlinear) stiffness matrices at various load levels below the limit point, is alternative to the perturbation-method-based procedure of Haftka, et al.[3]

The report is organized as follows. The general form of finite element force-displacement relationships and of the resulting equations which describe the behavior of the complete structure is given in Section II. It is presumed that a displacement (stiffness) method of analysis is employed in description of the complete system. The approach to determination of the nonlinear pre-buckling behavior, through a direct

iterative procedure, is presented in Section III. Both first-order and second-order iterative schemes are presented. Section IV is devoted to an examination of the relationship between the load intensity and the determinant of the system stiffness matrix and the use of this data in the calculation of the bifurcation load intensity.

The approach to postbuckling analysis, through application of a perturbation technique, is described in Section V and the extension of this approach to cope with initial imperfections is given in Section VI. Section VII is devoted to an exposition of the method for limit point determination for perfect structures.

Three problems are solved in Section VIII in verification of the present approach and for the purpose of comparison with other methods. The first problem is that of the shallow arch. This case, for which an exact solution is available, illustrates the use of the direct iteration - interpolation method in determination of the bifurcation point following upon a nonlinear fundamental path and demonstrates the prediction of behavior for both perfect and imperfect forms of the arch by use of the perturbation method.

The second problem concerns an axially-loaded beam on nonlinear elastic foundation. This structure evidences a linear (trivial) prebuckling behavior, but enables representation of a snap-through buckling phenomenon in the presence of initial imperfection of the beam. A number of alternative solution procedures are applied to this problem and are compared with the procedures devised in this report.

The third problem studied is a rectangular uniaxially compressed flat plate. The perfect flat plate possesses a trivial prebuckling displacement state for displacements normal to the plane of the plate and the bifurcation load is calculated accurately by linear theory. A postbuckling analysis is performed by means of the perturbation method, and the results are compared with a classical solution.

Details of the application of the procedures given in this report to the arch, beam and flat plate problems are described in the Appendix.

Although the problems solved are elementary from the standpoint of finite element representation, they delineate all features of the more complex situations and are among the few cases which have been studied thoroughly and for which comparison solutions or test data are available. Such comparisons were essential in a study addressed to a class of problems for which a multitude of alternative procedures have only recently been proposed.

Because of the scope and complexity of the present topic, emphasis is restricted to the basic aspects of finite element procedures for nonlinear prebuckling and initial postbuckling analysis. Note should be taken of at least two other critical and equally extensive aspects of the topic, computational efficiency and detailed formulation of finite element relationships per se. These and other facets of the total problem in practical application are excluded from consideration herein.

II. ELEMENT AND SYSTEM FORMULATIONS

The purpose of this section is to define the general form and characteristics of finite element stiffness formulations for geometrically nonlinear analysis. In accordance with the above-expressed intention to limit the scope of this report to the procedures for pre- and post-buckling analysis, no consideration is given to specific types of elements, fields for specific element representations, the selection of assumed stress or displacement, nor to the formulative procedures leading to the detailed finite element and system equations. The latter considerations are examined in reference 10.

In accordance with concepts detailed by Mallett and Marcal [16], the element stiffness equations for small strain nonincremental finite displacement analysis for conservative loadings and a Lagrangian frame of reference are of the general form

$$[k]\{\Delta\} + [n_1(\Delta)]\{\Delta\} + [n_2(\Delta)]\{\Delta\} = \lambda \{F\} \qquad (1)$$

where

$\lambda\{F\}$ and $\{\Delta\}$ are the applied loads and corresponding displacements (degrees-of-freedom), respectively. λ, the loading parameter, is a scale factor applied to the "normalized" load

vector {F}. The load vector {F} is normalized in the sense that it represents only the relative magnitude of the loads corresponding to the respective degrees-of-freedom {Δ}. Thus, the joint loads are applied in fixed proportion to one another.

[k] is the linear (small displacement theory) stiffness matrix.

$[n_1(\Delta)]$ is the first-order ("geometric") stiffness matrix, where the individual terms are linear functions of the degrees-of-freedom {Δ}. A simplified form of this matrix permits linear stability analysis, as in Euler buckling.

$[n_2(\Delta)]$ is the second-order ("geometric") stiffness matrix, with individual terms a quadric function of the degrees-of-freedom {Δ}. These terms arise from the components of strain energy which are the first derivatives of w with respect to the spatial variables raised to the fourth power.

Upon assembly of the element relationships defined by Eq. (1) to form a representation of the complete structure, (global representation) the following equations are obtained

$$[K]\{\Delta\} + [N_1(\Delta)]\{\Delta\} + [N_2(\Delta)]\{\Delta\} = \lambda\{P\} \qquad (2)$$

where the definitions of K, N_1, N_2 and P for the global representation correspond to those given above for k, n_1, n_2, and F for the respective elements.

In indicial notation, Equation (2) becomes

$$K_{ij}\Delta_j + N_{ijk}\Delta_j\Delta_k + N_{ijkl}\Delta_j\Delta_k\Delta_l = \lambda P_i \qquad (2a)$$

Indicial notation is especially useful in nonlinear finite element analysis since the constants of the problem (N_{ijk} and N_{ijkl}) are readily identified and can be stored permanently, in contrast to the matrix format where $[N_1(\Delta)]$ and $[N_2(\Delta)]$ are dependent on the displacements and change continually during the numerical analysis process. This aspect of detailed computation is discussed by Morin[10] and Vos[17]. It should also be noted that although one would not expect symmetry in the matrix forms of $[N_1(\Delta)]$ and $[N_2(\Delta)]$, a symmetric format of the matrix coefficients is achieved by proper manipulation of the basic forms of these matrices. The matrix (Eq. 2) and indicial

(Eq. 2a) notations will be employed interchangeably throughout this report.

III. PREBUCKLING ANALYSIS

A variety of methods for nonlinear equilibrium analysis have been explored in the literature; much of this work has been summarized by Haisler, et al.[18] A popular choice is the Newton-Raphson method[19] or its variants[20], due to a quadratic convergence property. The Newton-Raphson method will fail, however, at or in the vicinity of the bifurcation point. Although procedures have been devised to surmount this problem[21,22], they do not appear appropriate to the present overall approach. The direct iterative method, employed herein, presents no difficulty at the bifurcation point and is therefore chosen for performance of nonlinear prebuckling analysis.

In the direct iterative method, a solution to Equation (2) will already have been obtained at the load level $\{P^{i-1}\}$, with corresponding displacements $\{\Delta^{i-1}\}$, and the load is incremented by an amount $\{\Delta P\}$ to reach $\{P^i\}$. Thus, in the analysis at the load level $\{P^i\}$, the matrices $[N_1]$ and $[N_2]$ are formed on the basis of $\{\Delta^{i-1}\}$ and Equation (2) is written in the form

$$[K]\{\Delta^i\}^1 = \lambda\{P^i\} - [N_1(\Delta^{i-1})]\{\Delta^{i-1}\} - [N_2(\Delta^{i-1})]\{\Delta^{i-1}\} \quad (3)$$

where the superscript 1 on $\{\Delta^i\}$ indicates the first solution in the iterative determination of $\{\Delta^i\}$ solving

$$\{\Delta^i\}^1 = [K]^{-1}\{\lambda\{P^i\}-[N_1(\Delta^{i-1})]\{\Delta^{i-1}\}-[N_2(\Delta^{i-1})]\{\Delta^{i-1}\}\} \quad (4)$$

We then form

$$[K]\{\Delta^i\}^2 = \lambda\{P^i\} - [N_1(\Delta^i)^1]\{\Delta^i\}^1 - [N_2(\Delta^i)^1]\{\Delta^i\}^1 \quad (3a)$$

which can be solved for $\{\Delta^i\}^2$. In the general (j^{th}) iterative solution

$$[K]\{\Delta^i\}^j = \lambda\{P^i\} - [N_1(\Delta^i)^{j-1}]\{\Delta^i\}^{j-1} - [N_2(\Delta^i)^{j-1}]\{\Delta^i\}^{j-1} \quad (3b)$$

The iterative sequence continues until $\{\Delta^i\}^j$ is within $\{\Delta^i\}^{j-1}$ to a specified tolerance. It should be noted that direct iteration requires only the inversion of the linear stiffness matrix and continued re-formation of $[N_1]$ and $[N_2]$.

The proof of convergence of this approach below the bifurcation point is given in Reference 12.

Difficulties are encountered in this approach when the nonlinearities are severe. Such difficulties are often manifested by continued iteration in a loop about the convergent solution. In such cases an improved procedure is to employ a higher-order iterative scheme, which is obtained by substituting Equation (3a) into Equation (3). The result, for the j^{th} iteration, is of the form

$$[K]\{\Delta^i\}^j = \lambda[\,[I] - [N_1][K]^{-1} - [N_2][K]^{-1}\,]\{P^i\} - [\,[N_1][K]^{-1}[N_1] + [N_1][K]^{-1}[N_2] + [N_2][K]^{-1}[N_1] + [N_2][K]^{-1}[N_2]\,]\{\Delta^i\}^{j-1} \qquad (5)$$

where $[N_1]$ and $[N_2]$ are formed on the basis of $\{\Delta^i\}^{j-1}$.

The knowledge of a nearby solution, as for $\{\Delta^{i-1}\}$ in Equation 3, enhances the efficiency of the iterative process. For this reason, the analysis is recommended to be performed at various load levels, extending from a level close to zero load through to a level somewhat beyond the bifurcation load.

IV. DETERMINATION OF BIFURCATION

The basis of the approach to determination of the first branching from the fundamental path (the bifurcation point) is the familiar stability condition that the second variation of the potential energy be zero at such a point. The equilibrium equation (Equation 2) represents the first variation of the potential energy and by applying the second variation one obtains the following condition at $\lambda = \lambda^c$

$$\text{Det} = |\,[K] + 2\,[N_1(\Delta)] + 3\,[N_2(\Delta)]\,| = 0 \qquad (6)$$

where Det symbolizes the determinant of the indicated matrix. The factors 2 and 3 on $[N_1]$ and $[N_2]$ arise from imposition of the second variation; this can be seen from the indicial form, Equation 2a, which is in effect subjected to a differentiation with respect to Δ_r ($r = i,j,k,\ell$) in application of the variation.

Figure 2 illustrates the manner in which the above condition is employed in identification of the bifurcation point. Figure 2a shows a representative load-parameter-displacement (λ-Δ) plot while Figure 2b shows the corresponding variation of Det with λ. Thus, Det > 0 for $0 < \lambda < \lambda^c$ and Det < 0 for $\lambda > \lambda^c$. By establishing m solution points to either side of λ^c, Lagrange interpolation can be invoked to produce an expression for

$$\lambda = \sum_{i=1}^{m} \left(\prod_{j=1,\ j=i+1}^{i-1,\ m} \frac{\text{Det}-\text{Det}_j}{\text{Det}_j-\text{Det}_i} \right) \lambda_i \qquad (7)$$

where Det_i and λ_i denote the corresponding values at the ith load level. From Eq. (7), the bifurcation load λ^c is calculated by setting Det=0, i.e.

$$\lambda^c = \lambda \Big|_{\text{Det}\,=\,0}$$

Since the displacements and their derivatives at λ^c are needed for determination of the postbuckling path, they are also calculated by interpolation.

$$\Delta_i(\lambda) = \sum_{j=1}^{m} \left(\prod_{k=1,\ k=j+1}^{j-1,\ m} \frac{\lambda-\lambda_k}{\lambda_k-\lambda_j} \right) \Delta_i^j \qquad (8)$$

where Δ_i^j denotes the value of Δ_i at the jth load level λ_j. Then the desired displacements Δ_i^c are found by setting $\lambda=\lambda^c$. The derivatives of Δ_i are found by direct differentiation of Eq. (8) with respect to λ and evaluation at λ^c.

V. POSTBUCKLING ANALYSIS

The approach to postbuckling analysis is through application of a method in the class of "static perturbation" techniques.[7] The analysis furnishes the shape of the initial postbuckling path through the critical point using, as basic data, the load parameter at bifurcation (λ^c), the displacement vector of the fundamental path at bifurcation ($\{\Delta^c\}$) and derivatives of the latter with respect to the load parameter.

Figure 3 illustrates in a representative λ-Δ space the circumstance where a single postbuckling path emanates from the first critical point. In establishing an analytical description of this path we describe the displacement state by means of a

"sliding coordinate"[8] representation

$$\{\Delta\} = \{\bar{\Delta}\} + \{\Delta^p\} \tag{9}$$

where now $\{\bar{\Delta}\}$ describes displacements on the fundamental path and $\{\Delta^p\}$ gives the displacements on the postbuckling path with the fundamental path as a reference base. Thus, a mapping of the postbuckling behavior in $\lambda - \{\Delta^p\}$ space is effected with $\{\bar{\Delta}\} = 0$.

To obtain the equilibrium equation in terms of the new coordinates, we substitute Equation (9) into Equation (2). To designate this operation it is convenient to revert to indicial notation with $\{\Delta\} = \Delta_j$, $\{\bar{\Delta}\} = \bar{\Delta}_j$ and $\{\Delta^p\} = \Delta^p_j$ since in effecting the products $\Delta_j\Delta_k$ and $\Delta_j\Delta_k\Delta_\ell$ the term $\Delta_j = (\bar{\Delta}_j + \Delta^p_j)$ can be treated as a binomial in conventional manner. Thus we have

$$K_{ij}\bar{\Delta}_j + K_{ij}\Delta^p_j + N_{ijk}(\bar{\Delta}_j + \Delta^p_j)(\bar{\Delta}_k + \Delta^p_k) + N_{ijk\ell}(\bar{\Delta}_j + \Delta^p_j)(\bar{\Delta}_k + \Delta^p_k)(\bar{\Delta}_\ell + \Delta^p_\ell) = \lambda P_i \tag{10}$$

and, expanding and collecting multipliers of Δ^p_j

$$(K_{ij}\bar{\Delta}_j + N_{ijk}\bar{\Delta}_j\bar{\Delta}_k + N_{ijk\ell}\bar{\Delta}_j\bar{\Delta}_k\bar{\Delta}_\ell - \lambda P_i) + (K_{ij} + 2N_{ijk}\bar{\Delta}_k + 3N_{ijk\ell}\bar{\Delta}_k\bar{\Delta}_\ell)\Delta^p_j + (N_{ijk} + 3N_{ijk\ell}\bar{\Delta}_\ell)\Delta^p_j\Delta^p_k + N_{ijk\ell}\Delta^p_j\Delta^p_k\Delta^p_\ell = 0 \tag{11}$$

Since the fundamental path satisfies Equation (2), however, the first term in parentheses equals zero. Hence, the equilibrium equation in the new coordinates is given by

$$(K_{ij} + 2N_{ijk}\bar{\Delta}_k + N_{ijk\ell}\bar{\Delta}_k\bar{\Delta}_\ell)\Delta^p_j + (N_{ijk} + 3N_{ijk\ell}\bar{\Delta}_\ell)\Delta^p_j\Delta^p_k + N_{ijk\ell}\Delta^p_j\Delta^p_k\Delta^p_\ell = 0 \tag{12}$$

Although previously described computations (Section III) describe the fundamental path by discrete solution points, an analytical representation is now necessary. Thus, a Taylor series expansion about the bifurcation point is invoked:

$$\bar{\Delta} = \{\bar{\Delta}^c\} + (\lambda-\lambda^c)\{\bar{\Delta}'^c\} + \frac{1}{2}(\lambda-\lambda^c)^2\{\bar{\Delta}''^c\} + \ldots \tag{13}$$

This expression must next be substituted into Equation 12. In order to describe this development in specific terms, the decision is made to truncate the series at the indicated (third) term. Also, after substitution, terms higher than third order in Δ_i^p or the product of Δ_i^p and $(\lambda-\lambda^c)$ are discarded. Hence, after substitution, we obtain

$$[\bar{K}_{ij} + \bar{K}'_{ij}(\lambda-\lambda^c)+\bar{K}''_{ij}(\lambda-\lambda^c)^2]\Delta_j^p + (\bar{N}_{ijk} + \bar{N}'_{ijk}(\lambda-\lambda^c))\Delta_j^p\,\Delta_k^p + N_{ijk\ell}\,\Delta_j^p\,\Delta_k^p\,\Delta_\ell^p = 0 \qquad (14)$$

where

$$\bar{K}_{ij} = K_{ij} + 2N_{ijk}\,\bar{\Delta}_k^c + 3N_{ijk\ell}\,\bar{\Delta}_k^c\,\bar{\Delta}_\ell^c$$

$$\bar{K}'_{ij} = 2N_{ijk}\,\bar{\Delta}_k'^c + 6N_{ijk\ell}\,\bar{\Delta}_k'^c\,\bar{\Delta}_\ell^c$$

$$\bar{K}''_{ij} = N_{ijk}\,\bar{\Delta}_k''^c + 3N_{ijk\ell}(\bar{\Delta}_k'^c\,\bar{\Delta}_\ell'^c + \bar{\Delta}_k^c\,\bar{\Delta}_\ell''^c)$$

$$\bar{N}_{ijk} = N_{ijk} + 3N_{ijk\ell}\,\bar{\Delta}_\ell^c$$

$$\bar{N}'_{ijk} = 3N_{ijk\ell}\,\bar{\Delta}_\ell^c \qquad (15)$$

Description of the postbuckling path will now be accomplished, also as a series, but in the form

$$\{\Delta^p\} = \varepsilon\{q_1\} + \varepsilon^2\{q_2\} + \varepsilon^3\{q_3\} + \ldots. \qquad (16)$$

where $\{q_1\}$, $\{q_2\}$, $\{q_3\}$, etc. are displacement modes with additional properties as described in the development to follow. The scalar value ε is the path parameter with meaning defined later. An expansion of the load parameter in the post buckling regime is also required

$$\lambda-\lambda^c = \varepsilon\Gamma_1 + \varepsilon^2\Gamma_2 + \varepsilon^3\Gamma_3 + \ldots \qquad (17)$$

Where Γ_1, etc. are values to be determined.

At this juncture it is of interest to note the contrast with the conventional procedure in structural analysis, where an expansion is employed only for the independent variable, such as $\{\Delta\}$, and a solution is obtained for this variable for given λ. The solution process will involve incrementation of ε, from which both $\{\Delta\}$ and λ will be evaluated.

Substituting Equations (16) and (17) into Equation (14) and collecting like powers of ε yields

$$\varepsilon\,(\bar{K}_{ij}\,q_{j_1}) + \varepsilon^2(\bar{K}_{ij}\,q_{j_2} + \bar{K}_{ij}\,\Gamma_1\,q_{j_1} + \bar{N}_{ijk}\,q_{j_1}\,q_{k_1})$$

$$+ \varepsilon^3\,(\bar{K}'_{ij}\,\Gamma_2\,q_{j_1} + \bar{K}_{ij}\,q_{j_3} + \bar{K}'_{ij}\,\Gamma_1\,q_{j_2} + \bar{K}''_{ij}\,\Gamma_1^2\,q_{j_1} \qquad (18)$$

$$+ \bar{N}_{ijk}\,(q_{j_2}\,q_{k_1} + q_{j_1}\,q_{k_2}) + \bar{N}'_{ijk}\Gamma_1 q_{j_1} q_{k_1}) = 0$$

and, for $\varepsilon \neq 0$

$$\bar{K}_{ij}\,q_{j_1} = 0 \qquad (18a)$$

$$(\bar{K}_{ij}\,q_{j_2} + \bar{K}'_{ij}\,\Gamma_1\,q_{j_1} + \bar{N}_{ijk}\,q_{j_1}\,q_{k_1}) = 0 \qquad (18b)$$

$$(\bar{K}_{ij}\,q_{j_3} + \bar{K}'_{ij}(\Gamma_2 q_{j_1} + \Gamma_1\,q_{j_2}) + \bar{K}''_{ij}\Gamma_1^2\,q_{j_1} + 2\bar{N}_{ijk}q_{j_1}\,q_{k_2}$$

$$+ \bar{N}'_{ijk}\,\Gamma_1\,q_{j_1}\,q_{k_1} + N_{ijk\ell}\,q_{j_1}q_{k_1}q_{\ell_1}) = 0 \qquad (18c)$$

It is important to distinguish between $\{\bar{\Delta}^c\}$ and $\{q_1\}$. The former represents the displaced state of the fundamental path ($\{\Delta^p\} = 0$) at the bifurcation point while the latter is the eigenvector of the postbuckling path at the same point. Indeed, $\{\bar{\Delta}^c\}$ is employed in the formation of $\bar{K}_{ij}$.

Before considering the solution of (18a) to obtain q_{j_1} it must be noted that the rank of Equations 18a, 18b and 18c is n-1, where n is the total number of degrees-of-freedom j = 1,...n. To deal with factors related to this circumstance, we designate ε as one of the node point displacements, say Δ_1^p. We can employ degree-of-freedom 1 without loss of generality since it is always possible to rearrange the equations so that a chosen degree-of-freedom appears in the first location. The chosen degree-of-freedom is generally the displacement at a prominent point, say the transverse displacement at the center of a beam.

With $\varepsilon = \Delta_1^p$, in order for Equation 16 to hold, we must have $q_{12} = q_{13} = q_{14} = 0$, etc., so that Equation 16 may now

be written (in expanded form)

$$\begin{Bmatrix} \Delta_1^p \\ \Delta_2^p \\ \cdot \\ \cdot \\ \cdot \\ \Delta_n^p \end{Bmatrix} = \Delta_1^p \begin{Bmatrix} 1 \\ q_{2_1} \\ \cdot \\ \cdot \\ \cdot \\ q_{n_1} \end{Bmatrix} + (\Delta_1^p)^2 \begin{Bmatrix} 0 \\ q_{2_2} \\ \cdot \\ \cdot \\ \cdot \\ q_{n_2} \end{Bmatrix} + (\Delta_1^p)^3 \begin{Bmatrix} 0 \\ q_{2_3} \\ \cdot \\ \cdot \\ \cdot \\ q_{n_3} \end{Bmatrix} + \ldots \qquad (16a)$$

We may now return to determination of q_{j_1} ($= \{q_1\} = \lfloor 1\ q_{2_1} \ldots q_{n_1} \rfloor^T$). From (18a), it is clear that $\{q_1\}$ is the eigenvector of $[\bar{K}_{ij}]$, normalized on q_{1_1} (see Equation (16a)).

Next, Γ_1 is evaluated using Equation (18b). To accomplish this, premultiply the equation by q_{j_1} and rearrange

$$q_{j_1}\ \bar{K}_{ij}\ q_{j_2} = -\left(\bar{K}'_{ij}\ q_{j_1}\Gamma_1 + N_{ijk}\ q_{j_1}\ q_{k_1}\right) q_{i_1}$$

Since $q_{j_1}\ \bar{K}_{ij}$ is zero (Equation 18a), the left side is zero. By solution of the remainder

$$\Gamma_1 = -\frac{N_{ijk}\ q_{i_1}\ q_{j_1}\ q_{k_1}}{\bar{K}'_{ij}\ q_{i_1}\ q_{j_1}} \qquad (19)$$

Substituting this result into Equation (18b), there is obtained

$$\bar{K}_{ij}\ q_{j_2} = \bar{N}_{ijk}\ q_{j_1}\ q_{k_1} - \left(\frac{N_{ijk}\ q_{i_1}\ q_{j_1}\ q_{k_1}}{\bar{K}'_{ij}\ q_{i_1} q_{j_1}}\right) \bar{K}'_{ij}\ q_{j_1} \qquad (20)$$

The rank of this system of equations is n-1, but it is recalled from the above that $q_{1_1} = 1$ and $q_{1_2} = 0$, and by imposition of these conditions Equation (20) may be solved to yield q_{j_2}.

Similarly, we multiply Eq. (18c) by q_{i_1} to yield

$$\Gamma_1\ \bar{K}'_{ij}\ q_{i_1} q_{j_2} + \Gamma_2\ \bar{K}'_{ij}\ q_{i_1} q_{j_1} + \Gamma_1^2\ \bar{K}''_{ij}\ q_{i_1} q_{j_1} + 2\bar{N}_{ijk} q_{j_1} q_{k_2} q_{k_1}$$

$$+ \Gamma_1\ \bar{N}'_{ijk}\ q_{i_1} q_{j_1} q_{k_1} + N_{ijk\ell}\ q_{i_1} q_{j_1} q_{k_1} q_{\ell_1} = 0$$

From which,

$$\Gamma_2 = \frac{-1}{\bar{K}'_{ij} q_{i_1} q_{j_1}} (\Gamma_1 \bar{K}'_{ij} q_{i_1} q_{j_2} + \Gamma_1^2 \bar{K}''_{ij} q_{i_1} q_{j_1} + 2\bar{N}_{ijk} q_{i_1} q_{j_1} q_{k_2}$$

$$+ \Gamma_1 \bar{N}'_{ijk} q_{i_1} q_{j_1} q_{k_1} + N_{ijk\ell} q_{i_1} q_{j_1} q_{k_1} q_{\ell_1}) \qquad (21)$$

and, q_{i_3} can be determined accordingly

Continued application of the above procedure would permit development of terms to any order in Equations (16) and (17). To synthesize the present results for the first two terms of Equation (17)

$$\lambda - \lambda^c = \Delta_1^p \left(\frac{-D_1}{D_2}\right) - (\Delta_1^p)^2 \frac{1}{D_2}\left(-\frac{D_1}{D_2} \cdot D_3 + \frac{D_1^2}{D_2^2} D_4 + D_5 - \frac{D_1}{D_2} D_6 + D_7\right) \qquad (22)$$

where the scalars D_1, ... D_7 are (using Eqs. 15)

$$D_1 = \bar{N}_{ijk} q_{i_1} q_{j_1} q_{k_1}$$

$$D_2 = \bar{K}'_{ij} q_{i_1} q_{j_1}$$

$$D_3 = \bar{K}'_{ij} q_{i_1} q_{j_2}$$

$$D_4 = \bar{K}''_{ij} q_{i_1} q_{j_1}$$

$$D_5 = 2\bar{N}_{ijk} q_{i_1} q_{j_1} q_{k_2}$$

$$D_6 = \bar{N}'_{ijk} q_{i_1} q_{j_1} q_{k_1} = 3N_{ijk\ell} \bar{\Delta}^c_\ell q_{i_1} q_{j_1} q_{k_1}$$

$$D_7 = N_{ijk\ell} q_{i_1} q_{j_1} q_{k_1} q_{\ell_1} \qquad (23)$$

Equations (16a) and (22) are the desired post-buckling load-displacement relations. Note that more complex forms could have been obtained by choosing more terms.

VI. EFFECT OF IMPERFECTION

In the presence of geometric imperfection or loading eccentricity the behavior of the true structure differs from that of the idealized perfect structure and additional terms must be added to Equation (2), the equilibrium equation. Consistent with Koiter's approach to this problem, we choose here to describe the imperfections in the form of a vector $\gamma\{I\}$ (γI_i in indicial notation), where γ is the magnitude of the imperfection and $\{I\}$ is a vector of relative nodal imperfections, i.e., a listing of the initial displacements at the respective degrees-of-freedom but in normalized form. Furthermore, we multiply the vector of imperfections by the loading parameter λ and treat the result as an "equivalent loading". Thus, the equilibrium equations are now

$$K_{ij}\Delta_j + N_{ijk}\Delta_j\Delta_k + N_{ijk\ell}\Delta_j\Delta_k\Delta_\ell = \lambda P_i + \lambda\gamma I_i \tag{24}$$

The approach to the solution of the above equations follows closely to that of the preceding section. With the introduction of the sliding coordinate, Equation 11 becomes

$$(K_{ij} + 2N_{ijk}\bar{\Delta}_k + 3N_{ijk\ell}\bar{\Delta}_k\bar{\Delta}_\ell)\,\Delta_j^p + (N_{ijk}+3N_{ijk\ell}\bar{\Delta}_\ell)\Delta_j^p\Delta_k^p + N_{ijk}\Delta_j^p\Delta_k^p\Delta_\ell^p = \lambda\gamma I_i \tag{25}$$

To proceed as before, the fundamental path is again expanded into a Taylor series as in Equation (13). Upon substitution of this Taylor series into the equation (25), one obtains in place of Equation 14

$$[\bar{K}_{ij} + \bar{K}'_{ij}(\lambda-\lambda^c) + \bar{K}''_{ij}(\lambda-\lambda^c)^2]\,\Delta_j^p + (\bar{N}_{ijk} + N'_{ijk}(\lambda-\lambda^c))\Delta_j^p\Delta_k^p + N_{ijk\ell}\,\Delta_j^p\Delta_k^p\Delta_\ell^p = \lambda\gamma I_i \tag{26}$$

Now, the series expansions of Δ_i^p and $(\lambda-\lambda^c)$ (Equations 16 and 17) are again employed. These are substituted into Equation (26) and in the grouping of terms the term $\lambda\gamma I_i$ is assigned to the group of terms of order ε^2. Then, the resulting equations are

$$\bar{K}_{ij}\, q_{j_1} = 0 \tag{27a}$$

$$\bar{K}_{ij}\, q_{j_2} + \bar{K}'_{ij}\, \Gamma_1\, q_{j_1} + \bar{N}_{ijk}\, q_{j_1} q_{k_1} - \left(\frac{\lambda\gamma}{\epsilon^2}\right) I_i = 0 \tag{27b}$$

$$\bar{K}_{ij}\, q_{j_3} + \bar{K}'(\Gamma_2\, q_{j_1} + \Gamma_1\, q_{j_2}) + \bar{K}''_{ij}\, \Gamma_1^2\, q_{j_1} + 2N_{ijk}\, q_{j_1} q_{k_2} + \bar{N}'_{ijk}\, \Gamma_1\, q_{j_1} q_{k_1} + N_{ijk\ell}\, q_{j_1} q_{k_1} q_{\ell_1} = 0 \tag{27c}$$

Again q_{j_1} (= $\{q_1\}$) is the eigenvector of $\bar{K}_{ij}$. To determine Γ_1 we also adopt the procedure used previously in conjunction with Equation (18b) and multiply $\{q_1\}$ into Equation (27b). One obtains

$$\Gamma_1\, \bar{K}'_{ij}\, q_{i_1} q_{j_1} + \bar{N}_{ijk}\, q_{i_1} q_{j_1} q_{k_1} - \frac{\lambda\gamma}{\epsilon^2}\, I_i\, q_{i_1} = 0$$

$$\text{or} \quad \Gamma_1 = \frac{\bar{N}_{ijk} q_{i_1} q_{j_1} q_{k_1} + \frac{\lambda\gamma}{\epsilon^2} I_1 q_{i_1}}{\bar{K}'_{ij}\, q_{i_1} q_{j_1}} = \frac{-D_1}{D_2} + \frac{\lambda\gamma}{\epsilon^2}\, \frac{I_i q_{i_1}}{D_2} \tag{28}$$

and, by substitution of this expression for Γ_1 into Equation (27b), there is obtained

$$q_{j_2} = q_{j_{21}} + q_{j_{22}}\, \frac{\lambda\gamma}{\epsilon^2} \tag{29}$$

where $q_{j_{21}}$ and $q_{j_{22}}$ are the solutions of the following equations:

$$\bar{K}_{ij}\, q_{j_{21}} = \frac{D_1}{D_2}\, \bar{K}'_{ij}\, q_{j_1} - \bar{N}_{ijk}\, q_{j_1}\, q_{k_1} \tag{29a}$$

$$\bar{K}_{ij}\, q_{j_{22}} = -\frac{I_i q_i}{D_2}\, \bar{K}'_{ij}\, q_{j_1} + I_i \tag{29b}$$

Note that $q_{j_{21}}$ is identical to q_{j_2} in the postbuckling analysis of the perfect structure. Again, $q_{j_{21}}$ and $q_{j_{22}}$ are determined to within one arbitrary constant and the condition $q_{1_{22}} = 0$ yields

$$q_{1_{21}} = 0, \quad q_{1_{22}} = 0$$

The value of Γ_2 is determined from Equation 27c, as before, by multiplying the latter by $\{q_1\}$. The resulting equation is

identical to that previously given and by substitution of Equation (27c) and solution for Γ_2 there is obtained

$$\Gamma_2 = -\frac{1}{D_2}\left[\left(D_3+D_{31}\frac{\lambda\gamma}{(\Delta_1^p)^2}\right)\Gamma_1 + D_4\,\Gamma_1^2 + D_5+D_{51}\frac{\lambda\gamma}{(\Delta_1^p)^2} + \Gamma_1 D_6+D_7\right] \tag{30}$$

where $D_{31} = \bar{K}'_{ij}\, q_{i_1}\, q_{i_{22}}$ and $D_{51} = 2\bar{N}_{ijk} q_{k_1} q_{j_1} q_{k_{22}}$. We now obtain specific formulas for the postbuckling path by substituting $\varepsilon = \Delta_1^p$ and the solutions for Γ_1, Γ_2, q_{i_1} and q_{i_2} into Equations (16) and (17). There results

$$\Delta_i^p = \Delta_1^p \cdot q_{i_1} + (\Delta_1^p)^2\, q_{i_{21}} + \lambda\gamma\, q_{i_{22}} \tag{31}$$

and

$$\begin{aligned}\lambda-\lambda^c = {} & \left(\frac{\lambda\gamma I_i q_{i_1}}{D_2}\right)^2 \frac{D_4}{D_2}\cdot(\Delta_1^p)^{-2} - \frac{D_{31}}{D_2}\frac{\lambda^2\gamma^2 I_i q_{i_1}}{D_2}(\Delta_1^p)^{-2} \\ & + \left(\frac{\lambda\gamma I_i q_{i_1}}{D_2}\right)(\Delta_1^p)^{-1} - \frac{1}{D_2}\left(\frac{\lambda\gamma I_i q_{i_1}}{D_2}\right)\left(D_3+D_6 - \frac{D_1\cdot D_4}{D_2} + \frac{D_{51}}{I_i q_{i_1}} - \frac{D_1\cdot D_{31}}{I_i q_{i_1}}\right) \\ & - \frac{D_1}{D_2}\Delta_1^p - (\Delta_1^p)^2\frac{1}{D_2}\left[-\frac{D_1}{D_2}(D_3+D_6) + \left(\frac{D_1}{D_2}\right)^2\cdot D_4+D_5+D_7\right]\end{aligned} \tag{32}$$

Since $\gamma I_i q_{i_1}$ is small and λ is of the same order as Δ_1^p when Δ_s^p is small, the first two terms in the right are of the order of $(\gamma I_i q_{i_1})^2$ and therefore can be neglected. Equation (34) then reduces to

$$\begin{aligned}\lambda-\lambda^c = {} & \frac{\lambda\gamma I_i q_{i_1}}{\Delta_1^p\cdot D_2} - \frac{\lambda\gamma I_i q_{i_1}}{D_2^2}\left(D_3+D_6 - \frac{D_1\cdot D_4}{D_2} + \frac{D_{51}}{I_i q_{i_1}} - \frac{D_1\cdot D_{31}}{D_2\cdot I_i q_{i_1}}\right) - \frac{D_1}{D_2}\Delta_1^p \\ & - \frac{(\Delta_1^p)^2}{D_2}\left[-\frac{D_1}{D_2}(D_3+D_6) + \left(\frac{D_1}{D_2}\right)^2 D_4+D_5+D_7\right]\end{aligned} \tag{33}$$

Equations (31) and (33) constitute the load-displacement relation. The limit point can be determined from a plot of this relation.

VII. EXTRAPOLATION METHOD FOR CALCULATION OF LIMIT POINT

In practical applications to structures without defined initial imperfections the analyst does not know in advance whether bifurcation will occur, in which case the foregoing procedures apply, or if a snap-through limit point situation (Figure 1c) will be encountered. In either case the advance along the fundamental path from the initiation of loading will progress towards a stiffness matrix with zero determinant, since this condition applies equally well to bifurcation and limit points. For snap-through, however, the analysis for the first load level beyond the limit point will yield a meaningless displacement vector.

With this information, the analyst identifies the possibility of a snap through situation and may attempt definition of the load intensity and the displacement vector at the limit point by an extrapolation of the data obtained at the already-obtained solution points below the limit point. As indicated above, the determinant of the total stiffness matrix is zero at the limit point and in addition (see Figure 2b) there is a stationary point on the λ-Det relationship, i.e.

$$\frac{d\lambda}{d(\text{Det})} = 0 \tag{34}$$

A series representation of λ versus Det may be written in the form

$$\lambda = b_0 + b_1 (\text{Det}) + b_2 (\text{Det})^2 + \ldots + b_m (\text{Det})^m \tag{35}$$

where m is the number of fundamental-path solution points employed and $b_o \ldots b_m$ are coefficients to be determined. By application of Equation (34), $b_1 = 0$. Then, a system of simultaneous equations for calculation of b_o, b_2, ... b_m is established by evaluation of Equation (35) at each of the m points. E.g., at the typical point i on the fundamental path

$$\lambda_i = b_0 + b_2 (\text{Det})_i^2 + \ldots b_m (\text{Det})_i^m \tag{36}$$

This yields a system of m equations whose solution furnishes the coefficients b_0, b_2, ... b_m. The limit point is computed

by setting Det to zero in Equation (35). Thus, at the limit point, $\lambda = b_0$.

An alternative to the above is the procedure devised by Haftka, et al[3], in which the geometric nonlinearities ($[N_2]$) and all terms of $[N_1]$ except those associated with linear stability analysis are treated as initial imperfections in a perturbation analysis. If the nonlinearities are moderate throughout much of the prebuckling state a simple assessment of these "initial imperfections" at the respective load levels is sufficiently accurate and the procedure should be far more efficient than that which is given above. When the problem is highly nonlinear, however, the accurate determination of the "initial imperfections" requires the same effort as in the present method and it would appear that no advantages are gained by invoking a perturbation procedure.

Extension of the above concept to the case of a structure with initial imperfections is discussed in the Concluding Remarks (Section IX).

VIII. ILLUSTRATIVE EXAMPLES

1. Clamped Thin Shallow Circular Arch

Details of the solution procedure for this and the other two illustrative examples are presented in the Appendix. The present section is devoted to a general description of the respective problems and the significant aspects of the results obtained.

The first problem concerns instability of the thin shallow circular arch with clamped ends (Figure 4). This problem has drawn much attention in the literature of geometrically nonlinear and postbuckling analysis because it is perhaps the most sophisticated structure for which "exact" solutions have been obtained [14,24]. Our objective in performing this example is to verify the accuracy in determination of the bifurcation point following upon a nonlinear fundamental path by comparison with the exact solution, and to demonstrate prediction of behavior for both perfect and imperfect forms of the arch by use of the present perturbation method.

The geometry of the arch is characterized by the parameter $R\theta_o^2/h$ and this parameter also governs in part the form of buckling, i.e., snap-through or bifurcation. The dimensions chosen here yield a value of 10.0, the same value employed in Reference 14. The finite element representation consists of eight equally-spaced arch elements whose formulation is detailed in the Appendix.

In the case of uniform radial loading of intensity p_o, for the chosen geometric parameter, bifurcation occurs prior to snap-through as illustrated in Figure 5 by solid lines for the classical solution. Numerical results are also shown in this figure. The direct iterative scheme discussed in Section III is used to yield the solution points on the fundamental path as given by the circled points. Also, Figure 6 shows the calculated stability determinant at each load level. Lagrangian interpolation gives the bifurcation load $\lambda^c = 1.9075$, which is within 0.2% of the exact value.

The arch buckles into an asymmetric shape and postbuckling load-displacement behavior is represented by a straight line (Figure 5). The exact solution gives -3.851 as the slope of this line while the slope found by the present perturbation method is -3.925, an error of less than 2%. Thus, the present numerical method is in close agreement with all aspects of the classical solution. Solution efficiency considerations are discussed in the Appendix.

In order to examine the snap-through buckling case we add the effect of an applied moment at mid-span. Limit points corresponding to different magnitudes of this moment are determined by using the perturbation method and treating the moment as an imperfection. The resulting load-deflection curves are plotted in Figure 5 and the limit points vs. imperfection are plotted in Figure 7. No alternative solution is presently available for comparison.

2. Beam on Nonlinear Foundation

The problem considered here is an axially-loaded beam on a nonlinear elastic foundation (Figure 8). It is of interest

to note that this problem has been employed in the performance of probabilistic analyses of an infinite beam with random initial imperfections.[25] Here, the purpose of this example is the comparison of four different methods for determination of the limit point: (a) the present perturbation method, (b) extrapolation from the iterative solution (Section VII of this paper), (c) Thompson's "conventional" perturbation method[11] and (d) Thompson's improved perturbation method.[9]

The nonlinear foundation modulus for the beam is given by $k_1w - k_2w^2 - k_3w^3$, where w is the transverse displacement and k_1, k_2, and k_3 are spring constants. k_1 simulates the linear stiffness [k]; k_2 and k_3 yield matrix coefficients which correspond to the $[n_1]$ and $[n_2]$ geometric stiffness matrices, respectively. Five different combinations of these constants were employed for the subject numerical solutions, as follows:

		$k_1/EI/L^4$	$k_2/EI/L^5$	$k_3/EI/L^6$	$P_{cr}/EI/L^2$
CASE	I	16	0	16000	11.49
	II	160	0	80000	26.09
	III	16	500	0	11.49
	IV	16	500	-1000	11.49
	V	16	500	1000	11.49

In Cases I-III either k_2 or k_3 is set equal to zero to simulate cases where $[n_1]$ and $[n_2]$, respectively, are zero. Cases IV and V correspond to the general nonlinear finite element formulation of a non-symmetric structure. The above listing also gives the critical loads as found in Reference 26.

In each case (I-V) the initial deviation of the complete beam is assumed to be of the form $w_o = \frac{\gamma L}{100} \sin \frac{\pi X}{L}$, where the imperfection parameter takes on values 0.5, 1, 2, 3, 5, 6, 7, 8, 9 and 10. As in the first example, the finite element idealization consists of eight equal-length elements.

In the presence of imperfection, the axially loaded beam exhibits a snap-through type of buckling due to the continuously

weakening foundation modulus $k_1w - k_2w^2 - k_3w^3$. Figure 9 shows the foundation modulus for Cases I-III. A typical load-displacement plot is shown in Figure 10 for Case IV for values of $w_{o_{max}} = \frac{\gamma L}{100}$ of 0 and 1.0, demonstrating the nature of this effect.

Curves of limit points vs. the imperfection amplitude $w_{o_{max}}$ are plotted in Figure 11 for Cases I-III. Close agreement between the two methods developed in this report (perturbation and determinant extrapolation) are observed, while the "conventional" perturbation method of Reference 11 produces larger error with larger imperfection. In using Thompson's improved perturbation method (Reference 9), the procedure involves the calculation of a single imperfection parameter on the basis of a preselected value of limit load. By taking the limit points computed in the present perturbation method as given input, the corresponding limit loads were calculated with the formulas in Reference 9. No significant differences from the present results were obtained so that the data given in Figure 11 for the "Perturbation" method can be taken to apply to both procedures.

For the more general cases (IV and V), with three non-zero spring constants, only the results of the present methods are available since no explicit formulas for these cases are available in References 9 and 11. The present results are given in Figure 12.

In using the extrapolation method in determination of the limit point as depicted in Figure 2, error estimation is in general not possible. The numerical results summarized in Table 1, however, show only a 5% maximum discrepancy between the extrapolated limit points and those obtained by the present perturbation method.

3. Flat Plate Post-Buckling

The final example refers to the postbuckling behavior of a perfectly flat simply-supported rectangular plate under uniaxial compression (Figure 13). The plate is assumed to be free to displace in its own plane. This problem possesses a trivial prebuckling displacement state (for transverse displace-

TABLE 1: BEAM ON NONLINEAR ELASTIC FOUNDATION. VALUES OF NORMALIZED LIMIT POINTS (λ_u/λ_c) VERSUS $W_{o_{max}}$

		$W_{o_{max}} = \frac{100\gamma}{L}$											
	*	0	0.5	1	2	3	4	5	6	7	8	9	10
I	a	1		0.679	0.553	0.475	0.417	0.375	0.338	0.308	0.287	0.263	0.248
	b	1	0.779	0.680	0.555	0.475		0.372	0.336	0.308	0.284	0.263	0.243
	c	1	0.739	0.585	0.342	0.136		-0.213	-0.370	-0.519	-0.660	-0.794	-0.925
II	a	1		0.599	0.470	0.384	0.330	0.291	0.256	0.236	0.216	0.198	0.182
	b	1	0.725	0.611	0.477	0.395		0.297	0.264	0.239	0.218	0.200	0.185
	c	1	0.659	0.459	0.142	-0.123		-0.577	-0.782	-0.975	-1.160	-1.330	-1.522
III	a	1		0.679	0.571	0.510	0.461	0.423	0.389	0.368	0.343	0.325	0.307
	b	1	0.761	0.680	0.582	0.517		0.431	0.399	0.374	0.351	0.332	0.313
	c	1	0.728	0.614	0.458	0.329		0.134	0.053	-0.024	-0.094	-0.161	-0.224
IV	a	1		0.665	0.556	0.495		0.403	0.354	0.347	0.325	0.305	0.287
	b	1	0.752	0.669	0.566	0.499		0.410	0.379	0.353	0.329	0.309	0.291
V	a	1		0.695	0.588	0.537		0.455	0.428	0.388	0.384	0.363	0.348
	b	1	0.765	0.690	0.598	0.538		0.460	0.431	0.407	0.387	0.368	0.352

*SOLUTION PROCEDURES:

a: Extrapolation Method (present report)

b: Perturbation Method (present report)

c: Method of Ref. 9.

ments), the bifurcation load is calculated accurately by use of linear theory, and because theoretical solutions[27,28] are available for postbuckling behavior. It has been chosen for analysis in this study for the sake of comparison of the perturbation method with the latter and because it introduces the finite element modeling of a continuum structure (a plate) as opposed to the finite element modeling of discrete structures (beams, arches) as in the preceding examples.

The analysis of the problem is performed with use of one element, representing a quadrant of the plate. The bifurcation point, calculated in a linear stability analysis, is found to be 36.29 lb./in., compared to the classical result[26] of 36.11 lb./in. (0.5% error). The postbuckling path calculated by the present perturbation method is plotted in Figure 13, together with Coan's results[27]. The two solutions are in close agreement.

IX. CONCLUDING REMARKS

Procedures for finite element analysis of geometrically nonlinear problems, extending over the prebuckling and initial postbuckling regimes, snap-through buckling, and accounting for initial imperfections, have been presented. These procedures fall into two general categories: a perturbation method and a method of determinant extrapolation.

The perturbation method corresponds closely to Thompson's procedure[9]; the methods differ in detailed application in the determination of limit points of imperfection-sensitive structures, where the present method is believed to furnish a more efficient route to the calculation of the limit point for given imperfection data. The method of determinant extrapolation, developed here only for the case of limit point analysis, is a new departure for the calculation of such points. The method is based upon a simpler algorithm than the perturbation approach, but is computationally more expensive in application.

Both approaches, as presented here, are quite limited in their range of representation of load-displacement behavior. By its nature, the perturbation method applies only in the vicinity of the first branching point. The determinant extrapolation point method does not extend beyond the limit point. It should be feasible to accomplish this extension by the decrementation of load upon reaching the limit point· this consideration is currently being explored. Another limitation, pertinent only to the perturbation approach, relates to stability phenomena with multiple branching paths at the first branching point. A classical example of this situation occurs in the buckling of an axially-compressed cylinder when the pre-buckling state is linear. Extensions of the present perturbation method to this condition are also in progress.

All computations of the fundamental path (or pre-limit-point path in the case of the determinant extrapolation method) were performed with use of a direct-iteration algorithm. As the survey by Haisler, et al[18] has shown, this algorithm has not been favored by other analysts dealing with the subject

problem. This is apparently due to the relative inefficiency of the method in comparison with alternatives, e.g., Newton-Raphson iteration. A higher-order direct iterative scheme was discussed herein but was not applied to the problems analyzed. The accuracy of the subject procedures was verified by solution of a series of problems. These problems are of quite simple form when measured against practical design analysis situations, but are nevertheless relatively complex from the standpoint of numerical computations because of the complexity of the phenomena represented. Also, these problems have been employed in studies of procedures alternative to the subject procedure and therefore represent a useful basis of comparison. A computer program for shell stability analysis has been developed as part of the present work; results of this effort are described in Reference 30.

The relative efficiency and accuracy of the subject procedures and various alternative approaches (e.g., references 3, 9, 10) remain open questions. In view of the inability of analysts to agree upon the optimum procedures in the restricted area of nonlinear prebuckling analysis, as disclosed in the survey of Reference 18, it is unrealistic to expect the definition of the most appropriate approach to postbuckling analysis at the present time. These measures will be obtained only after significant experience in practical application is recorded.

APPENDIX

SOLUTION DETAILS FOR ILLUSTRATIVE EXAMPLES

1. Clamped Thin Shallow Circular Arch Under Uniform Load

The state of strain in this structure (see Figure A-1) is completely described by the axial strain of the neutral axis, ε_θ, for which the strain-displacement equation is

$$\varepsilon_\theta = \frac{1}{R}(w_{,\theta} - u) + \frac{1}{2R^2}(u_{,\theta})^2 \qquad \text{(A-1a)}$$

and the curvature of the neutral axis, κ,

$$\kappa = \frac{u_{,\theta\theta}}{R^2} \qquad \text{(A-1b)}$$

where the comma denotes differentiation, u and w are the radial and axial displacements, respectively, and R is the arch radius. With these expressions and for uniform radial loading of intensity p, the potential energy is

$$\Pi_p = \Pi_{p_1} + \Pi_{p_2} + \Pi_{p_3} \qquad \text{(A-2)}$$

where, for the ith individual finite element joining points i-1 and i (see Figure A-1).

$$\Pi_{p_1} = \frac{EA}{2R^3}\int_{\theta_{i-1}}^{\theta_i}[R^2(w_{,\theta} - u)^2 + (u_{,\theta\theta})^2]d\theta - \int_{\theta_{i-1}}^{\theta_i} pu\, R d\theta$$

$$\Pi_{p_2} = \frac{EA}{2R^3}\int_{\theta_{i-1}}^{\theta_i}(w_{,\theta} - u)(u_{,\theta})^2\, d\theta \qquad \text{(A-3)}$$

$$\Pi_{p_3} = \frac{EA}{8R^3}\int_{\theta_{i-1}}^{\theta_i}(u_{,\theta})^4\, d\theta$$

The finite element displacement functions are the same as used by Walker[29].

$$\begin{aligned} u &= u_o(1-10\xi^3+15\xi^4-6\xi^5)+u_o'(\xi-6\xi^3+8\xi^4-3\xi^5) \\ &\quad + u_o''\left(\tfrac{1}{2}\xi^2 - \tfrac{3}{2}\xi^3 + \tfrac{3}{2}\xi^4 - \tfrac{1}{2}\xi^5\right) \\ &\quad + u_1(10\xi^3 - 15\xi^4 + 6\xi^5) + u_1'(-4\xi^3 + 7\xi^4 - 3\xi^5) \\ &\quad + u_1''\left(\tfrac{1}{2}\xi^3 - \xi^4 + \tfrac{1}{2}\xi^5\right) \\ w &= w_o(1-3\xi^2 + 2\xi^3) + w_o'(\xi-2\xi^2 + \xi^3) + w_1(\xi\xi^2-2\xi^3) \\ &\quad w_1'(-\xi^2 + \xi^3) \end{aligned} \qquad \text{(A-4)}$$

where ξ goes from zero to one along the ith arch segment (Figure A-1).

Upon substitution of the above displacement functions into the energy expression (A-2) and performance of the usual procedure of integration and differentiation, one obtains the equilibrium equations in the following standard form

$$K_{ij}\Delta_j + N_{ijk}\Delta_j\Delta_k + N_{ijk\ell}\Delta_j\Delta_k\Delta_\ell = \lambda P_i \qquad \text{(A-5)}$$

Joint loads P_i are calculated on a "work-equivalent" basis.

For the specific problem under analysis, the properties of the arch are R = 10 in., h = 0.0684 in., θ_o = 15°, EA = 2.056 x 10^6 lb, EI = 796 lb. $in.^2$, so that the geometric parameter $R\theta_o^2/h$ = 10.

Solution of the problem, based on an 8-element representation, proceeds as follows for the "perfect" structure subjected only to uniform radial load p. First, the prebuckling path is determined by use of the iterative method described in Section III, with solutions obtained at dimensionless load levels $\lambda = p\,\frac{k^2h}{EI}$ = 1, 1.5, 1.8, 1.85, 1.90, 1.91, 1.95, 2.00, 2.05 and 2.10. The covergence criterion is defined as

$\left|\frac{\Delta_j^{i+1}-\Delta_j^i}{\Delta_j^i}\right| \leq \eta$ for all j. Four different values for η are used: 0.05, 0.01, 0.005 and 0.001. The number of iterative cycles needed to achieve convergence at each load level for each η are plotted in Fig. A-2. It is of interest to note that near the bifurcation point (λ = 1.9098) the number of cycles for convergence increases sharply. However, monotonic convergence is observed in all load levels below or above the bifurcation point.

Based on the converged solution for displacements, the determinant of the total stiffness matrix (Equation 6) is calculated, with results as shown in Figure 6. Then, using Equations 7 and 8, the bifurcation point, (λ^c), displacements ($\bar{\Delta}_i$) and their derivatives ($\bar{\Delta}_i'$, $\bar{\Delta}_i''$) at bifurcation point are

easily calculated. The value of λ^c is found to be 1.9075. Next, the representation of post-buckling behavior is established. After obtaining λ^c, $\bar{\Delta}_i$, $\bar{\Delta}_i'$ and $\bar{\Delta}_i''$, the values of the coefficient D_i's can be calculated easily using Equation (23). It is found that Δ_{i_1}, the bifurcation mode, is anti-symmetric about the mid-span and $D_1 = D_3 = D_6 = 0$. The path parameter ε is chosen to be the central slope Δ_s^p and due to the anti-symmetry of Δ_{i_1}, the central deflection $\Delta_{c1} = 0$. The load-central deflection relation is represented by

$$\Delta_c^p = (\Delta_s^p)^2 \cdot \Delta_{c2} \tag{A-6}$$

$$\lambda - \lambda^c = -(\Delta_s^p)^2 \frac{1}{D_2}(D_5 + D_7) \tag{A-7}$$

After elimination of $(\Delta_s^p)^2$, there is obtained

$$\Delta_c^p = -(\lambda - \lambda^c)\left(\frac{D_2}{D_5+D_7} \cdot \Delta_{c2}\right) \tag{A-8}$$

From this the slope of the $\Delta_i^p - \lambda$ relationship is obtained as

$$\frac{d(\Delta_c^p)}{d\lambda} = -\left(\frac{D_2}{D_5+D_7}\ \Delta_{c2}\right) = -4.361 \tag{A-9}$$

Since the total deflection $\Delta_c = \bar{\Delta}_c + \Delta_c^p$,

$$\frac{d\Delta_c}{d\lambda} = \frac{d\bar{\Delta}_c}{d\lambda} + \frac{d(\Delta_c^p)}{d\lambda} = -.436 - 4.361 = -3.925 \tag{A-10}$$

To simulate an imperfect structure, an asymmetric imperfection is introduced in the form of a couple acting at mid-span (Figure 14). The additional term in the equilibrium equation (A-5) is then $\lambda\gamma I_i$. The values of I_i's are zero except for $I_{19} = 1$. Calculation then proceeds along the line of Section VI. In addition to the coefficients calculated above for the perfect structure we find $D_{51} = 0$ and $\Delta_{c22} = 0$ in the central deflection. The load-central deflection relation is then

$$\Delta_c = \bar{\Delta}_c + (\Delta_s^p)^2{}_{c2} \tag{A-11}$$

$$\lambda - \lambda^c = \frac{\lambda\gamma I_i q_{i1}}{\Delta_s^p \cdot D_2} - \frac{(\Delta_s^p)^2}{D_2}(D_5+D_7) \tag{A-12}$$

Curves for $\gamma = 0.1$, 0.5, 1.0 and 1.5 are plotted in Fig. 5. The limit points non-dimensionalized to $\frac{\lambda_u}{\lambda^c}$ for $0.1 \leq \gamma \leq 1.5$ are plotted in Fig. 7.

2. Beam on Nonlinear Foundation

It is assumed that the beam sustains only flexural deformation. Thus, it can be shown that the potential energy in the presence of initial deviations w_o and with a nonlinear foundation modulus $k_1 w - k_2 w^2 - k_3 w^3$ is

$$\Pi_p = \frac{1}{2}\int_L \left(\frac{d^2w}{dx^2}\right) EI dx + \frac{1}{2} k_1 \int_L w^2 dx - \frac{k_2}{3}\int_L w^3 dx - \frac{1}{4} k_3 \int_L w^4 dx - \frac{\lambda}{2}\int_L \left[\left(\frac{dw}{dx}\right)^2 + 2\frac{dw}{dx}\frac{dw_o}{dx}\right] dx \quad \text{(A-13)}$$

Assuming the displacement function of an element as

$$w = \lfloor f_e \rfloor \{\Delta\} = \underline{\lfloor \xi^3 - 2\xi^2 + \xi \mid \xi^3 - \xi^2 \mid 2\xi^3 - 3\xi^2 + 1 \mid 3\xi^2 - 2\xi^3 \rfloor} \begin{Bmatrix} \ell\phi_1 \\ \ell\phi_2 \\ w_1 \\ w_2 \end{Bmatrix} \quad \text{(A-14)}$$

with $\xi = \frac{x}{\ell}$ and with w_o similarly represented as $\gamma \lfloor f_e \rfloor \{\Delta_o\}$, the total potential energy in matrix form can be written as

$$\Pi_p = \frac{1}{2}\lfloor \Delta \rfloor [k]\{\Delta\} + \frac{k_1}{2} \Delta\, [Z]\{\Delta\} - \frac{k_2}{3}\lfloor \Delta \rfloor [n_1(\Delta)]\{\Delta\} - \frac{k_3}{4}\lfloor \Delta\, [n_2(\Delta^2)]\{\Delta\} - \frac{1}{2}\lambda \lfloor \Delta \rfloor [n]\{\Delta\} - \frac{1}{2}\lambda\gamma \lfloor \Delta \rfloor [n]\{\Delta_o\} \quad \text{(A-15)}$$

where, for each element

$$[k] = EI \int_\ell \{f_e''\} \lfloor f_e'' \rfloor dx$$

$$[n] = \int_\ell \{f_e'\} \lfloor f_e' \rfloor dx$$

$$[Z] = \int_\ell \{f_e\} \lfloor f_e \rfloor dx \quad \text{(A-16)}$$

$$[n_1(\Delta)] = \int_\ell \{f_e\} \lfloor \Delta \rfloor \{f_e\} \{f_e\} dx$$

and $$[n_2(\Delta)] = \int_\ell (\{f_e\} \lfloor f_e \rfloor \{\Delta\}) \cdot (\lfloor \Delta \rfloor \{f_e\} \lfloor f_e \rfloor) dx$$

The potential energy of the full length of the beam is obtained by summing the element potential energies, resulting in

$$\Pi_p = \frac{1}{2}\lfloor\Delta\rfloor [K]\{\Delta\} + \frac{k_1}{2} \lfloor\Delta\rfloor[Z]\{\Delta\} - \frac{k_2}{3} \lfloor\Delta\rfloor[N_1(\Delta)]\{\Delta\}$$

$$- \frac{k_3}{4}\lfloor\Delta\rfloor[N_2(\Delta)\{\Delta\} - \frac{1}{2} \lambda \lfloor\Delta\rfloor[N]\{\Delta\} - \frac{1}{2} \lambda\gamma \lfloor\Delta\rfloor[N]\{\Delta_o\} \qquad \text{(A-17)}$$

From (A-17) the equilibrium equation is obtained

$$([K]+k_1[Z]- [N])\{\Delta\}-k_2[N_1(\Delta)]\{\Delta\}-k_3[N_2(\Delta^2)]\{\Delta\} = \gamma\lambda[N]\{\Delta_o\} \qquad \text{(A-18)}$$

which can be rewritten as (denoting λ^c the eigenvalue of $[K]+k_1[Z]-\lambda[N]$)

$$([K]+k_1[Z]-\lambda^c[N])\{\Delta\}-(\lambda-\lambda^c)[N]\{\Delta\}-k_2[N_1(\Delta)\{\Delta\}-k_3[N_2(\Delta^2)]$$

$$= \gamma\lambda[N]\{\Delta_o\} \qquad \text{(A-19)}$$

Since in this case the pre-buckling path is trivial, one can proceed to post-buckling and limit point analysis immediately and identify $\{\Delta\}$ to Δ_1^p's. A comparison with Equation (14) reveals that

$$\bar{K}_{ij} = K_{ij} + k_1 Z_{ij} - \lambda^c N_{ij},\ \bar{K}'_{ij} = -N_{ij},\ \bar{K}''_{ij} = 0$$

$$\bar{N}_{ijk}\Delta_j\Delta_k = - k_2 [N_1(\Delta)]_{ij}\Delta_j,\ \bar{N}_{ijk} = 0 \qquad \text{(A-20)}$$

$$N_{ijk\ell}\Delta_j\Delta_k\Delta_\ell = - k_3(N_2(\Delta^2))_{ij}\Delta_j \text{ and } I_i = N_{ij}\Delta_{oj}$$

Thus, the previously derived formulas can be applied directly to yield all required information.

Computations are performed for combinations of the parameters k_1, k_2, k_3:

$k_2 = 0,\ k_1 \neq 0,\ k_3 \neq 0$:

The load, structure and behavior are symmetric in the pre-buckled state. With the term $\frac{k_2}{3}\lfloor\Delta\rfloor[N_1(\Delta)\{\Delta\} = 0$ it is found from Equation 23 that

$D_1 = D_4 = D_5 = D_{51} = D_6 = 0$ and

$D_2 = (K_{ij} + k_1 Z_{ij} - \lambda^c N_{ij})\, q_{i_1} q_{j_1}$

$D_3 = - N_{ij}\, q_{i_1} q_{j_1}$

$D_{31} = - N_{ij}\, q_{i_1} q_{j_{22}}$

$D_7 = - k_3 \,(N_2(q_{k_1} q_{\ell_1}))_{ij}\, q_{i_1} q_{j_1}$

From computation, $D_3 = D_{31} = 0$. The path parameter ε is identified to the central deflection Δ_c. The post-buckling path therefore becomes

$$\lambda^c - \lambda = \frac{D_7}{D_2} \Delta_c^2 \qquad \text{(A-21)}$$

The load-displacement relation for the corresponding imperfect beam is

$$\lambda^c - \lambda = - \frac{\gamma \lambda I_i q_{i_1}}{D_2 \Delta_c} + \frac{D_7 \Delta_c^{\,2}}{D_2} \qquad \text{(A-22)}$$

The limit point is calculated using the following simple relation, which is obtained by taking $\frac{d\lambda}{d\Delta_c} = 0$ and using equation (A-22)

$$\gamma = - \frac{2}{3\sqrt{3}} \frac{D_2 (\lambda^c - \lambda)^{3/2}}{\lambda I_i q_{i_1} \sqrt{\frac{D_7}{D_2}}} \qquad \text{(A-23)}$$

$k_3 = 0$, asymmetric case:

In this case the structure or loading are not symmetric and the fourth order term in total energy expression is zero. Since D_7 is zero in this case, the term associated with ε^2 is also put to zero to give the same degree of accuracy. Hence, the post-buckling path takes the even simpler form:

$$\lambda - \lambda = \Delta_c D_1 / D_2 \qquad \text{(A-24)}$$

where $$D_1 = -k_2 \,[N_1(q_{k_1})]_{ij} q_{i_1} q_{j_1} \qquad \text{(A-25)}$$

The load-displacement relation for the imperfect beam is

$$\lambda^c-\lambda = \Delta_c \left(\frac{D_1}{D_2} - \frac{\gamma\lambda I_i q_{i_1}}{\Delta_c^2 D_2}\right) \qquad \text{(A-26)}$$

The limit point is related to the imperfection parameter γ by

$$\gamma = -\frac{(\lambda^c-\lambda)^2}{4\frac{D_1}{D_2}\frac{\lambda I_i q_{i_1}}{D_2}} \qquad \text{(A-27)}$$

$k_2 \neq 0$, $k_3 \neq 0$, asymmetric case:

This is the general case modeling the nonlinear geometric matrices N_1 and N_2. Only D_4 and D_6 equal zero in this case. From computation D_3, D_{31} and D_{51} are negligible.

Then
$$\lambda^c-\lambda = \Delta_c \frac{D_1}{D_2} + \frac{\Delta_c^2}{D_2}(D_5 + D_7) \qquad \text{(A-28)}$$

$$\lambda^c-\lambda = \frac{\Delta_c}{D_2}\left(D_1 - \frac{\gamma I_i q_{i_1}}{\Delta_c^2}\right) + \frac{\Delta_c^2}{D_2}(D_5+D_7) \qquad \text{(A-29)}$$

The limit points can be calculated from

$$\gamma = \frac{-D_2(\lambda^c-\lambda)\Delta_c + D_1\Delta_c^2 + (D_5+D_7)\Delta_c^3}{\lambda I_i q_{i_1}} \qquad \text{(A-30)}$$

with
$$\Delta_c = \frac{-D_1 \pm \sqrt{D_1^2 + d(\lambda^c-\lambda)(D_5+D_7)D_2}}{3(D_5+D_7)} \qquad \text{(A-31)}$$

3. Flat Plate Postbuckling

The rectangular plate element employed for these computations was originally formulated by Bogner, et al (Reference 31) for large displacement analysis of circular cylinders and has more recently been extended[30] to deal with more general shapes of shells. The formulation is based upon bicubic interpolation functions for the three displacement components. In the case of the uniaxially compressed flat plate without initial imperfections the resulting system stiffness matrix is of the form

$$\begin{bmatrix} K_{mm} & 0 \\ 0 & K_{bb} \end{bmatrix} \begin{Bmatrix} \Delta_m \\ \Delta_b \end{Bmatrix} + \begin{bmatrix} 0 & N_{1_{mb}} \\ N_{1_{bm}} & N_{1_{bb}} \end{bmatrix} \begin{Bmatrix} \Delta_m \\ \Delta_b \end{Bmatrix}$$

$$+ \begin{bmatrix} 0 & 0 \\ 0 & N_{2_{bb}} \end{bmatrix} \begin{Bmatrix} \Delta_m \\ \Delta_b \end{Bmatrix} = \lambda \begin{Bmatrix} p_m \\ 0 \end{Bmatrix} \qquad \text{(A-32)}$$

where the subscripts b and m designate bending and membrane action respectively. For pre-buckling and bifurcation the displacements $\{\Delta_b\}$ are zero. Thus, the solution for pre-buckling displacements is

$$\{\bar{\Delta}_m\} = \lambda \, [K_{mm}]^{-1} \, \{P_m\} \qquad \text{(A-33)}$$

and bifurcation is determined from the condition

$$\left| [K_{bb}] + \lambda^c [N_{1_{bb}}] \right| = 0 \qquad \text{(A-34)}$$

Upon calculation of λ^c and the associated eigenvector the post-buckling analysis proceeds via evaluation of the coefficients D_i of Equation 23. It is found that only D_2, D_5 and D_7 are nonzero, and for the central lateral displacement of the plate (Δ_c^p) as the reference displacement, the normalized form of Equation 22 can be written as

$$\lambda/\lambda_c = 1 - [D_2(D_5+D_7) \, h^2/\lambda^c] \, (\frac{\Delta_c^p}{h})^2 \qquad \text{(A-35)}$$

The post-buckling response, in terms of λ versus Δ_c^p, is calculated from this equation and is plotted in Figure 14.

REFERENCES

1. Gallagher, R. H., "Analysis of Plate and Shell Structures", Proc. of Conf. on Application of Finite Element Methods in Civil Engineering, Vanderbilt Univ., 1969.

2. Hutchinson, J. W. and Koiter, W. T., "Postbuckling Theory", Applied Mech. Reviews, Dec. 1970.

3. Haftka, R. T., Mallett, R. H. and Nachbar, W., "A Koiter-Type Method for Finite Element Analysis of Nonlinear Structural Behavior", AFFDL TR 70-130, V. 1, Nov. 1970.

4. Bienek, M., "Post-Critical Behavior", Introductory Report for Ninth Congress of IABSE, Amsterdam, May, 1972.

5. Koiter, W. T., "On the Stability of Elastic Equilibrium", Thesis, Delft, 1945.

6. Budiansky, B. and Hutchinson, J., "A Survey of Some Buckling Problems", AIAA Journal, Vol. 4, Sept. 1966, pp. 1505-1510.

7. Sewell, M. J., "A General Theory of Equilibrium Paths Through Critical Points", Proc. Royal Soc. A. 306, pp. 201-223, 1968.

8. Thompson, J. M. T., "A General Theory for the Equilibrium and Stability of Discrete Conservative Systems" ZAMP, Vol. 20, 1969.

9. Thompson, J. M. T., "A New Approach to Elastic Branching Analysis", J. Mech. Phys. Solids, V. 18, 1970.

10. Morin, N., "Nonlinear Analysis of Thin Shells", Report R70-43, Dept. of Civil Engrg., M.I.T., 1970.

11. Thompson, J. M. T. and Walker, A. C., "The Branching Analysis of Perfect and Imperfect Discrete Structural Systems", J. Mech. and Phys. Solids, V. 17, 1969.

12. Dupuis, G. A., Pfaffinger, D. and Marcal, P. V., "Effective Use of the Incremental Stiffness Matrices in Non-linear Geometric Analysis", IUTAM Symposium on High Speed Computing of Elastic Structures, Liege, Belgium, 1970.

13. Lang, T. E., "Post-Buckling Response of Structures Using the Finite Element Method", Ph.D. Thesis, Univ. of Washington, 1969.

14. Kerr, A. D. and Soifer, M. T., "The Linearization of the Prebuckling State and its Effect on the Determined Instability Load", Trans. ASME, Journal of Applied Mech., V. 36, pp. 775-783, 1969.

15. Stein, M., "Some Recent Advances in the Investigation of Shell Buckling", AIAA Journal, V. 6, No. 12, Dec. 1968, pp. 2339-2345.

16. Mallett, R. and Marcal, P. V., "Finite Element Analysis of Nonlinear Structures", Proc. ASCE, Journal of the Structural Div., V. 94, pp. 2081-2106, 1968.

17. Vos, Robert G., "Finite Element Analysis of Plate Buckling and Postbuckling", Ph.D. Thesis, Rice University, Houston, Texas, 1970.

18. Haisler, W.E., Stricklin, J. A. and Stebbins, F., "Development and Evaluation of Solution Procedures for Geometrically Nonlinear Structural Analysis by the Direct Stiffness Method" Proc. of AIAA/ASME 12th Structures, Structural Dynamics, and Materials Conf., Anaheim, Calif., April 1971.

19. Thurston, G. A., "Newton's Method Applied to Problems in Nonlinear Mechanics", Trans. ASME, Journal of Applied Mech., V. 32, pp. 383-388, 1965.

20. Zeleznik, F. J., "Quasi-Newton Methods for Nonlinear Equations", Journal of the ACM, V. 15, No. 2, April 1968.

21. Thurston, G., "Continuation of Newton's Method Through Bifurcation Points", Trans. ASME, Journal of Applied Mech., V. 91, pp. 425-430, 1969.

22. Bueckner, H. F., Johnson, M. W. and Moore, R. H., "The Calculation of Equilibrium States of Elastic Bodies by Newton's Method", Proc. Ninth Midwestern Mechanics Conf., Univ. of Wisc., Madison, Wisconsin, 1965, pp. 201-213.

23. Cohen, G. A., "Effect of a Nonlinear Prebuckling State on the Postbuckling Behavior and Imperfection Sensitivity of Elastic Structures", AIAA Journal, V. 6, No. 8, Aug. 1968, pp. 1616-1619.

24. Schreyer, H. L. and Masur, E. F., "Buckling of Shallow Arches", Proc. ASCE, Journal of the Engineering Mechanics Div., V. 92, No. EM4, pp. 1-20, Aug. 1966.

25. Fraser, W. B. and Budiansky, B., "The Buckling of a Column with Random Initial Deflections", Trans. ASME Journal of Applied Mech., June, 1969.

26. Timoshenko, S. and Gere, J. M., "Theory of Elastic Stability", 2nd Ed., McGraw-Hill Book Co., 1961.

27. Coan, J. M., "Large Deflection Theory for Plates with Small Initial Curvature Loaded in Edge Compression", J. Appl. Mech., V. 18, 1951.

28. Walker, A. C., "The Post-Buckling Behavior of Simply-Supported Square Plates", The Aeronautical Quarterly, V. XX, Aug. 1969.

29. Walker, A. C., "A Nonlinear Finite Element Analysis of Shallow Circular Arches", Int. Journal Solids Structures, V. 5, pp. 97-107, 1969.

30. Lien, S., "Finite Element Thin Shell Pre- and Post-Buckling Analysis", Ph.D. Thesis, Structural Engrg. Dept., Cornell University, 1971.

31. Bogner, F., Fox, R. and Schmit, L., "Finite Deflection Analysis Using Plate and Cylindrical Shell Discrete Elements", AIAA Journal, V. 6, No. 5, May 1968.

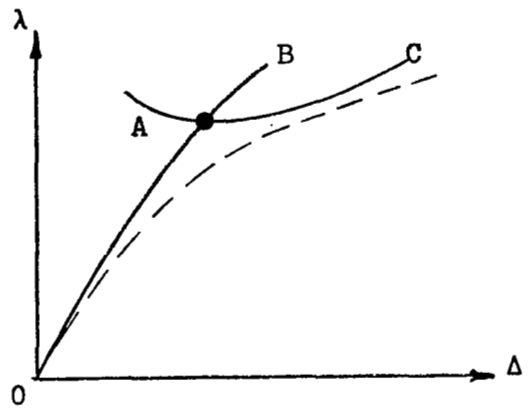

a. Bifurcation with Ascending Post-buckling Path

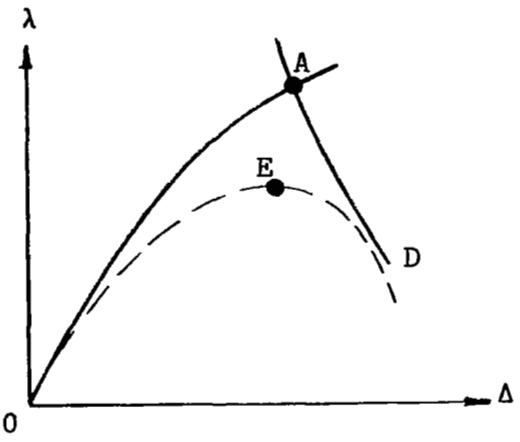

b. Bifurcation with Descending Post-buckling Path

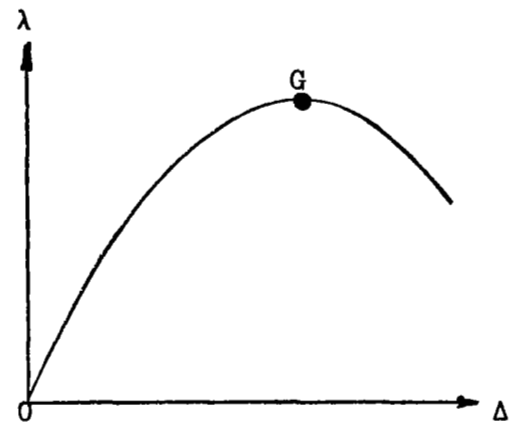

c. Limit Point-No Bifurcation

FIGURE 1. FORMS OF INSTABILITY UNDER STUDY

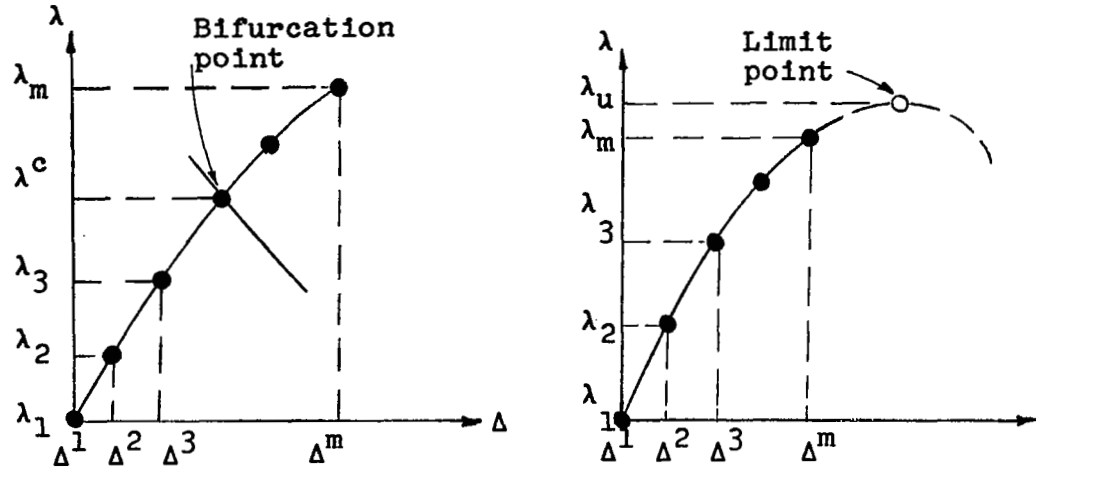

a. Load-Deflection Plots

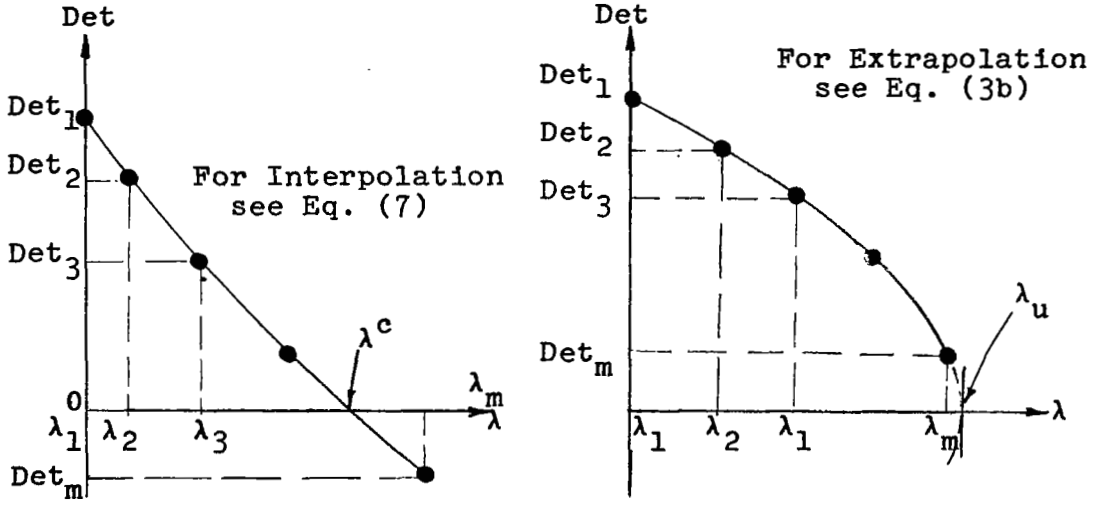

b. Load-Determinant Response

FIGURE 2. DETERMINATION OF BIFURCATION AND LIMIT POINTS BY INTERPOLATION AND EXTRAPOLATION OF LOAD-DETERMINANT RESPONSE.

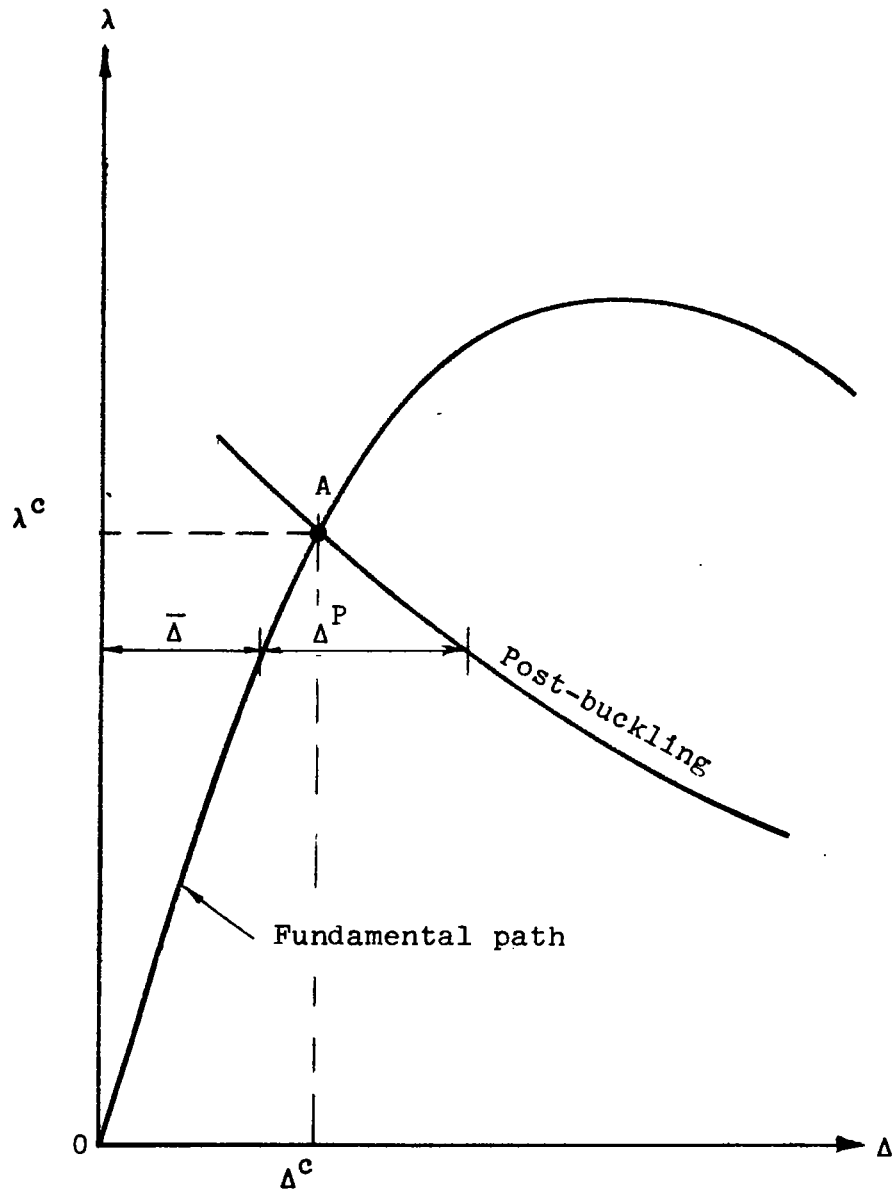

FIGURE 3. SLIDING COORDINATE SYSTEM

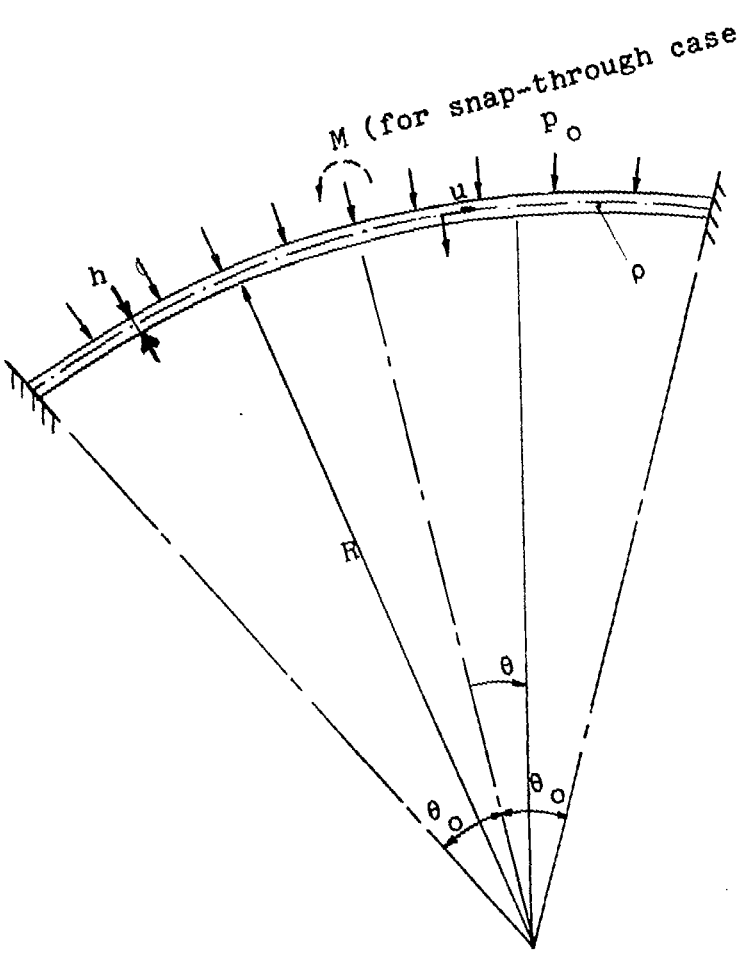

- GEOMETRY AND LOADING

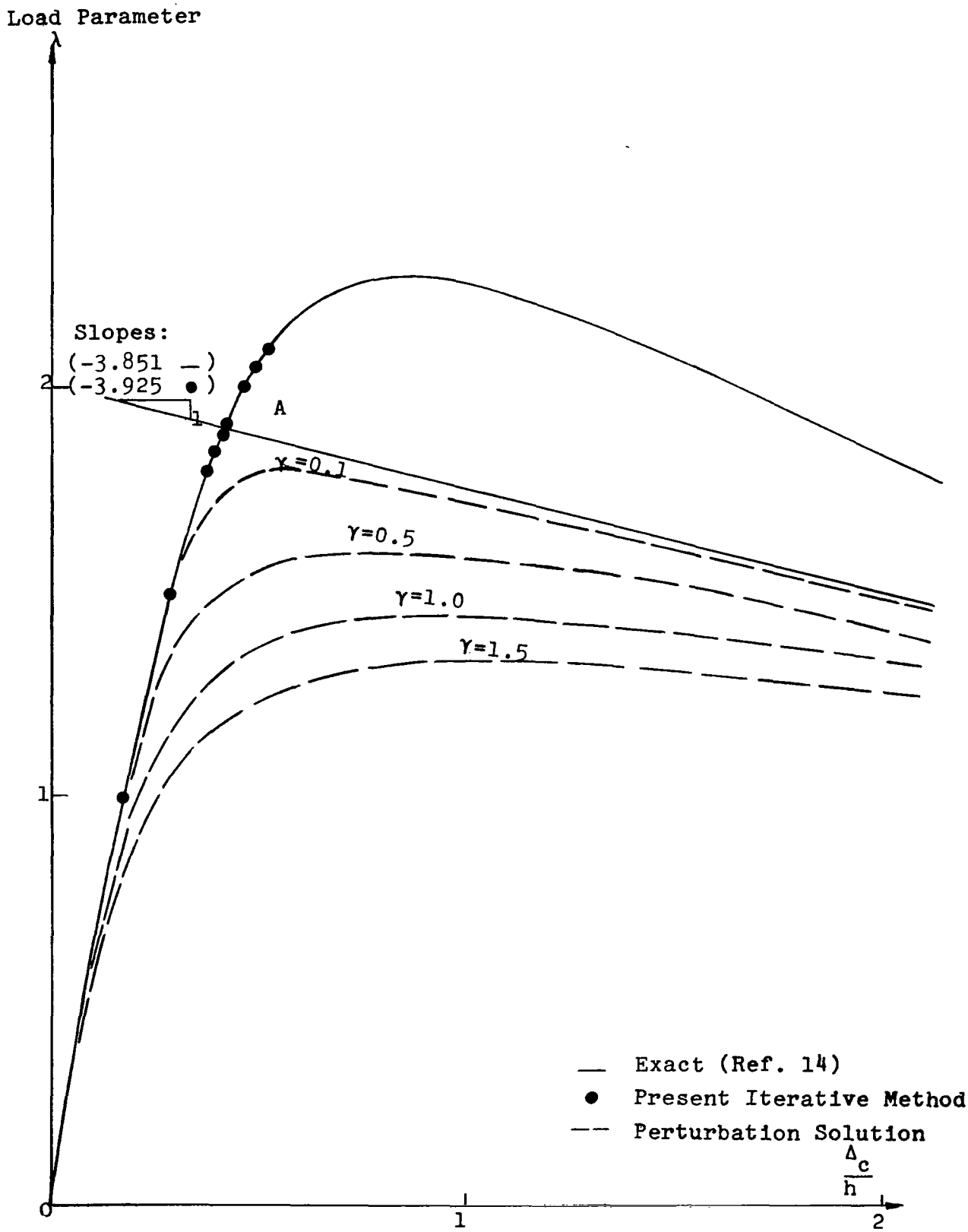

FIGURE 5. LOAD VS. CENTRAL DEFLECTION FOR PRE-BUCKLING, POST-BUCKLING AND IMPERFECT BEHAVIORS

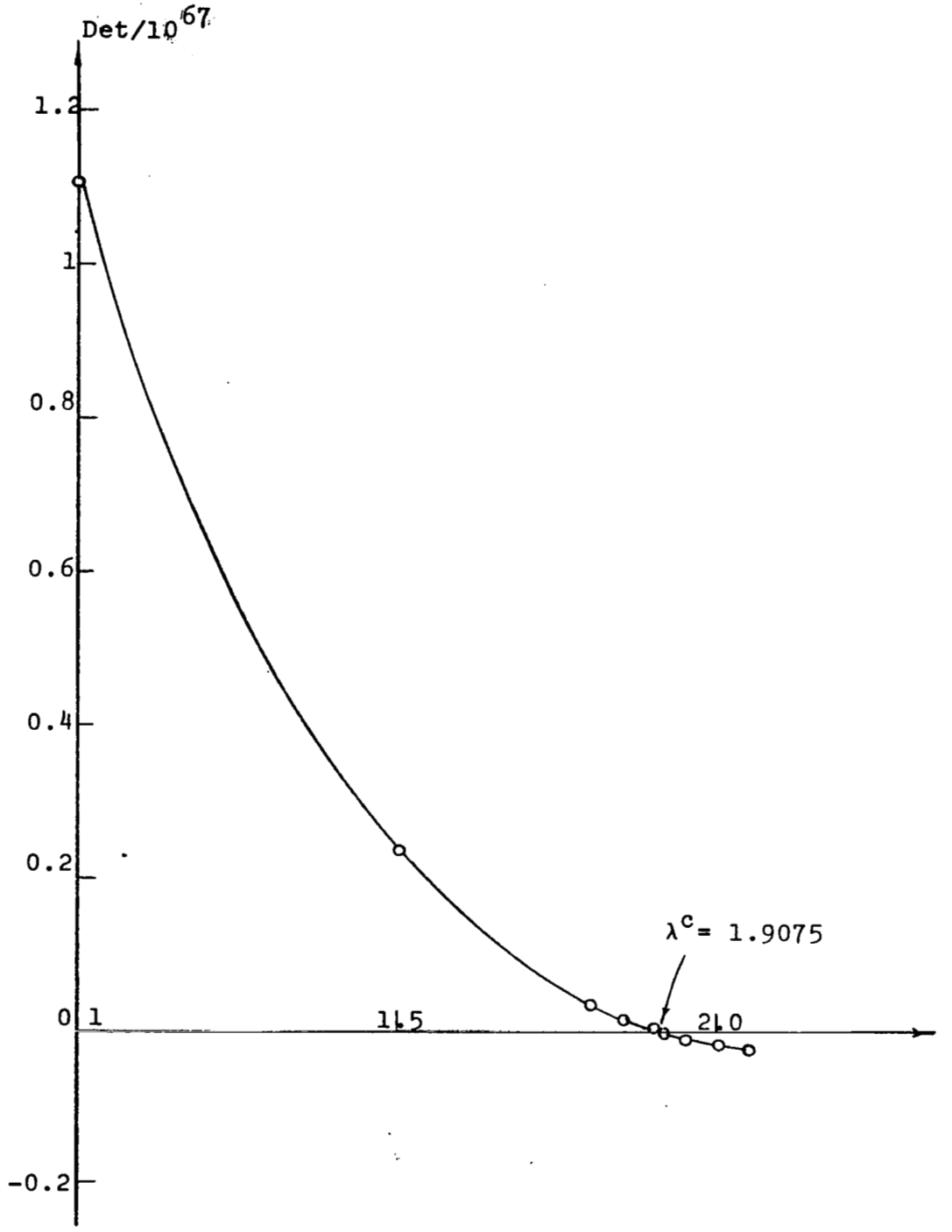

FIGURE 6. ARCH PROBLEM. INTERPOLATION FOR BIFURCATION POINT

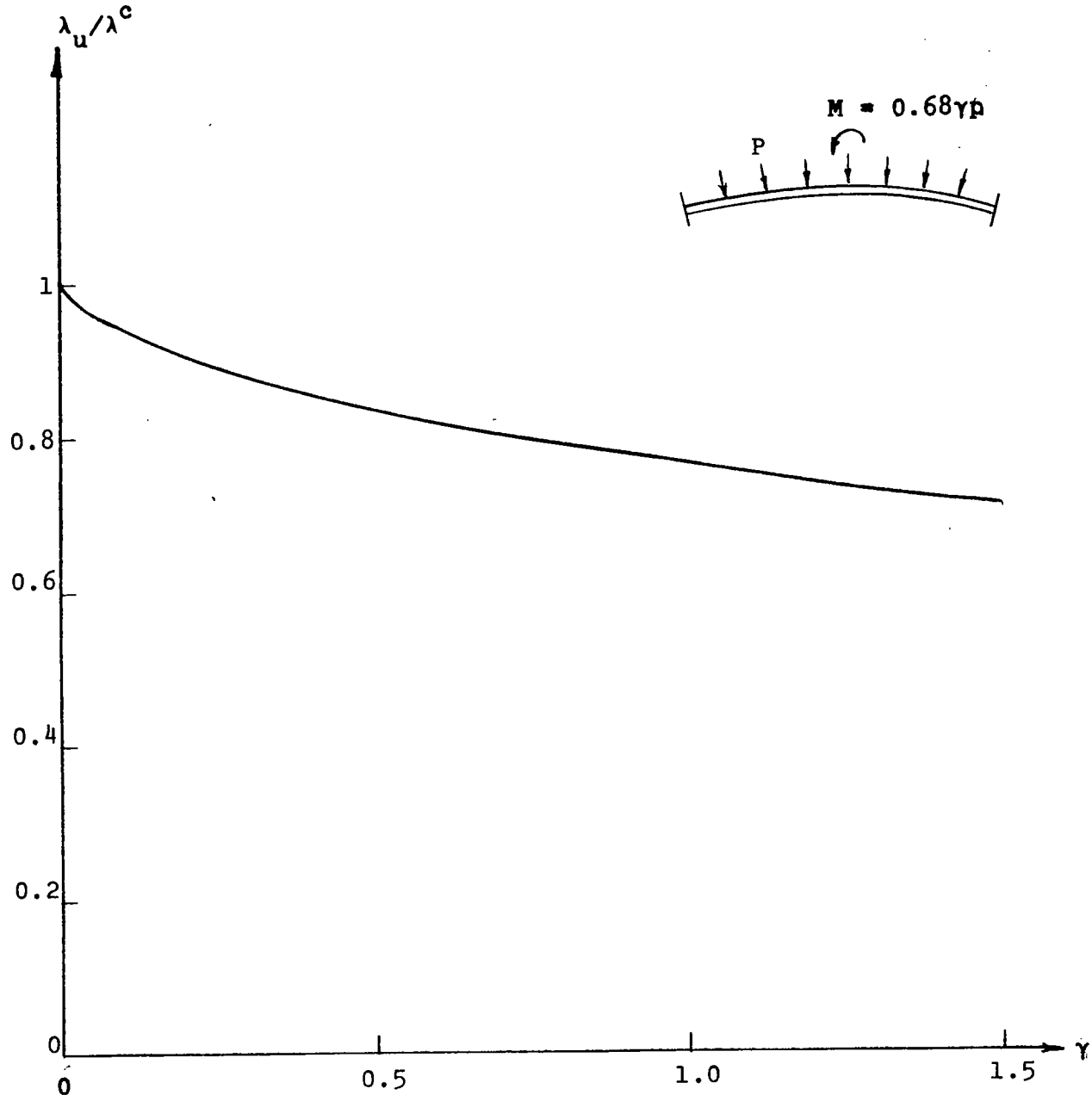

FIGURE 7. ARCH PROBLEM. LIMIT LOAD VERSUS IMPERFECTION

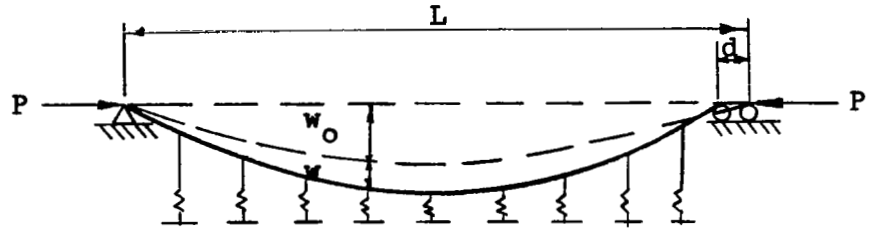

Foundation Force:

$$k_1 w - k_2 w^2 - k_3 w^3$$

$$w_o = \gamma \cdot \frac{L}{100} \sin \frac{x}{L}$$

FIGURE 8. BEAM ON NONLINEAR ELASTIC FOUNDATION

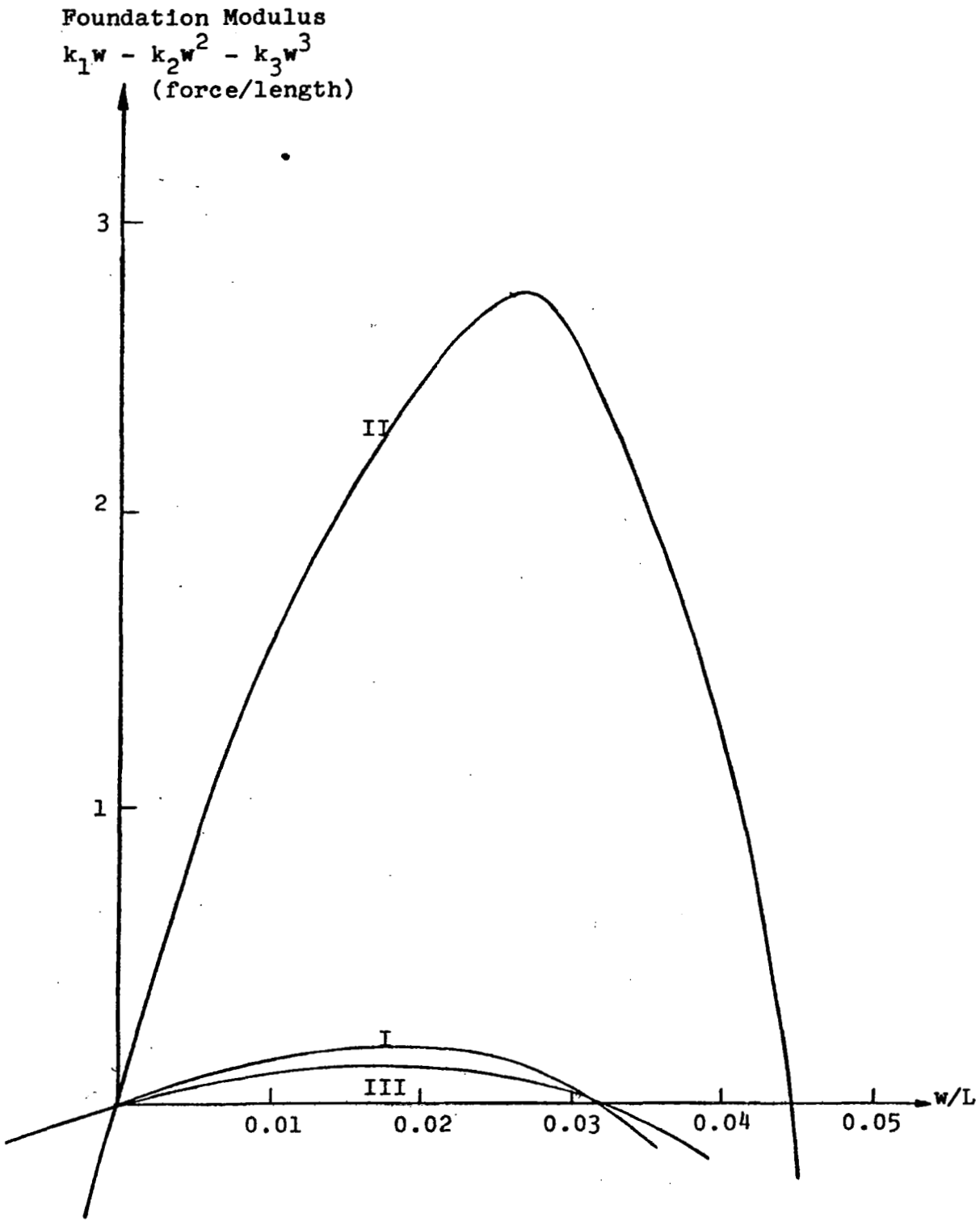

FIGURE 9. ELASTIC FOUNDATION PROPERTIES

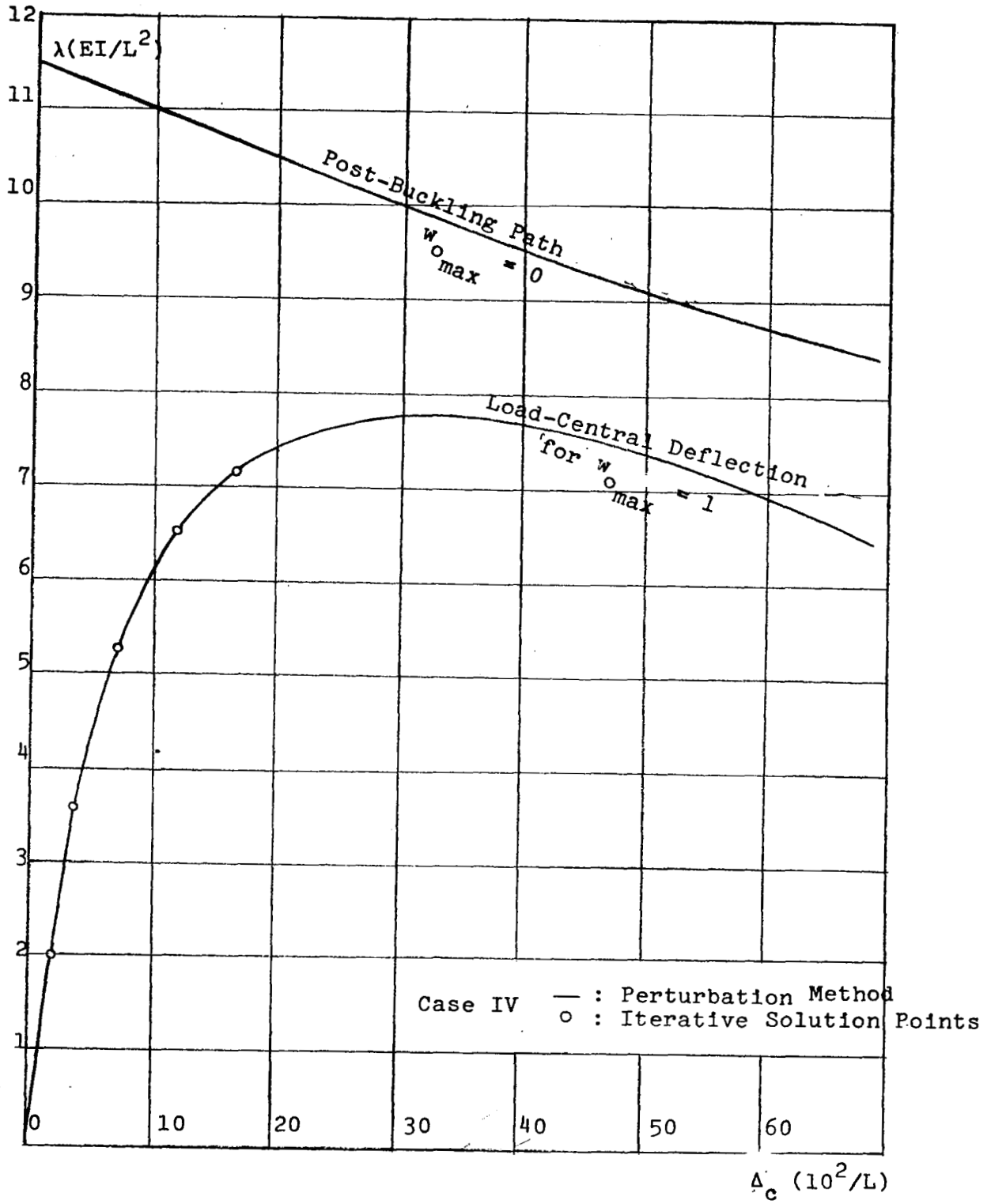

FIGURE 10. POST-BUCKLING PATH AND LOAD-DISPLACEMENT RELATIONSHIP.

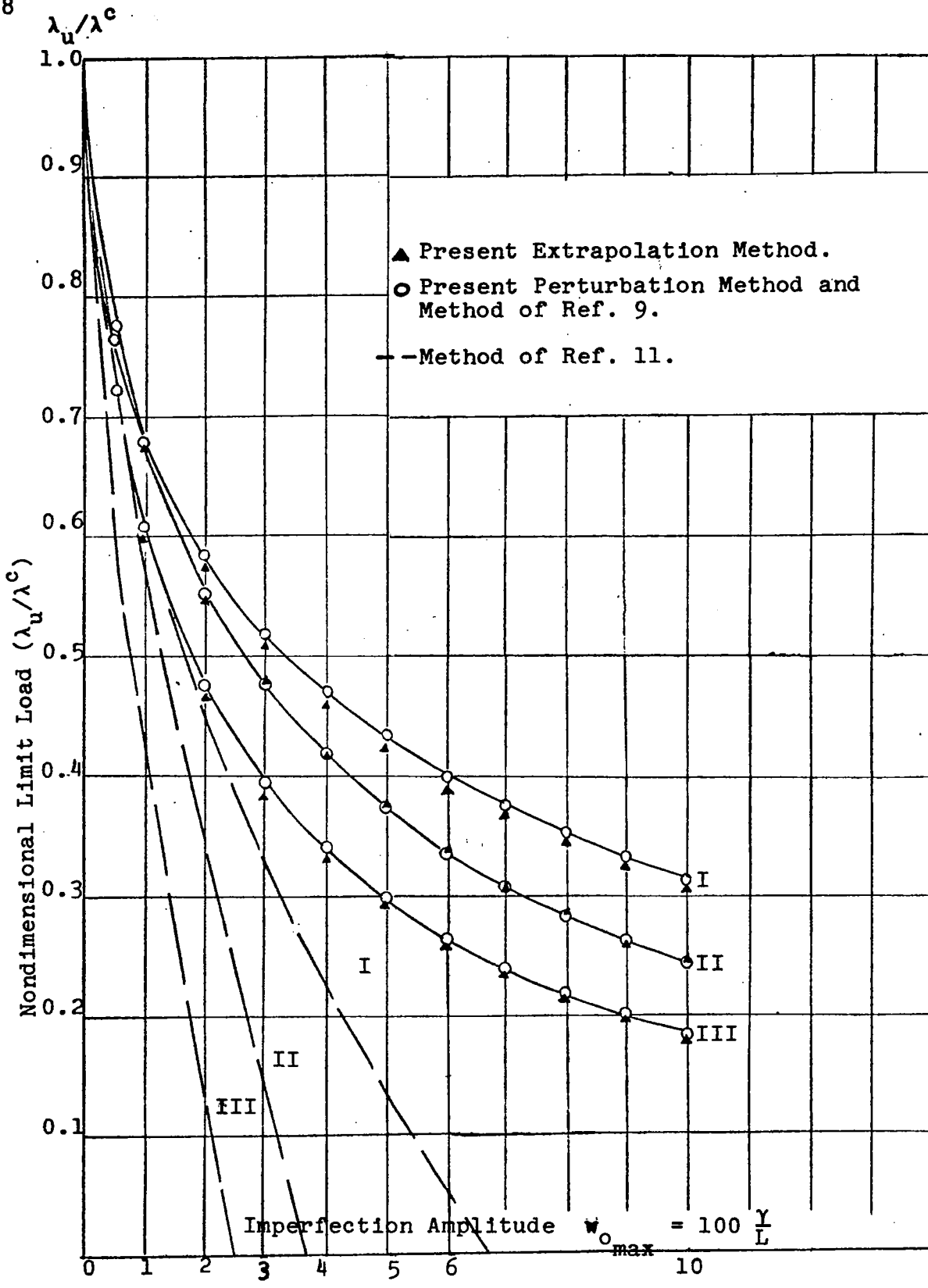

FIGURE 11. CASES I-III. LIMIT LOAD AS A FUNCTION OF $w_{o_{max}}$

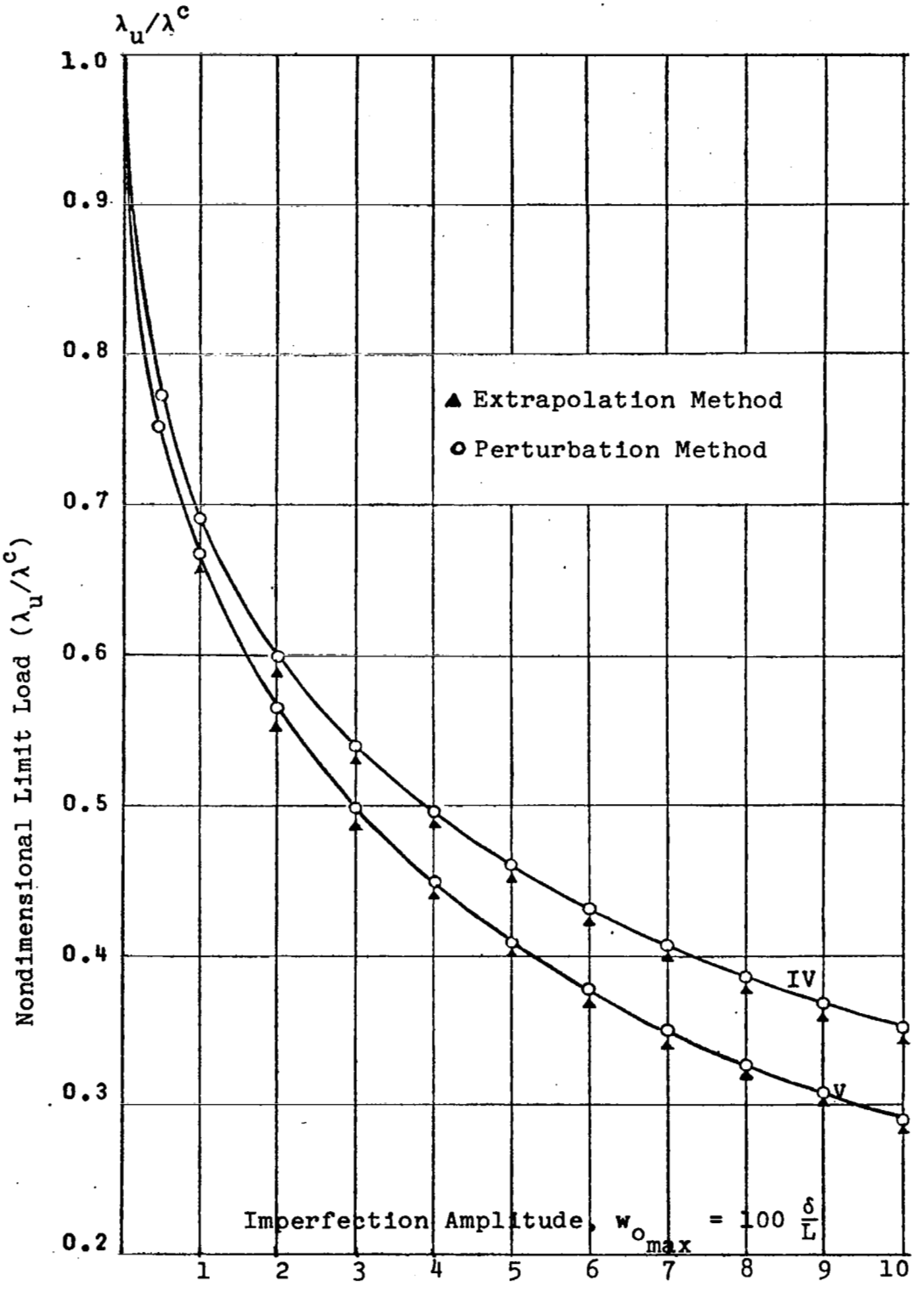

FIGURE 12. CASES IV, V. LIMIT LOAD AS A FUNCTION OF $w_{o_{max}}$

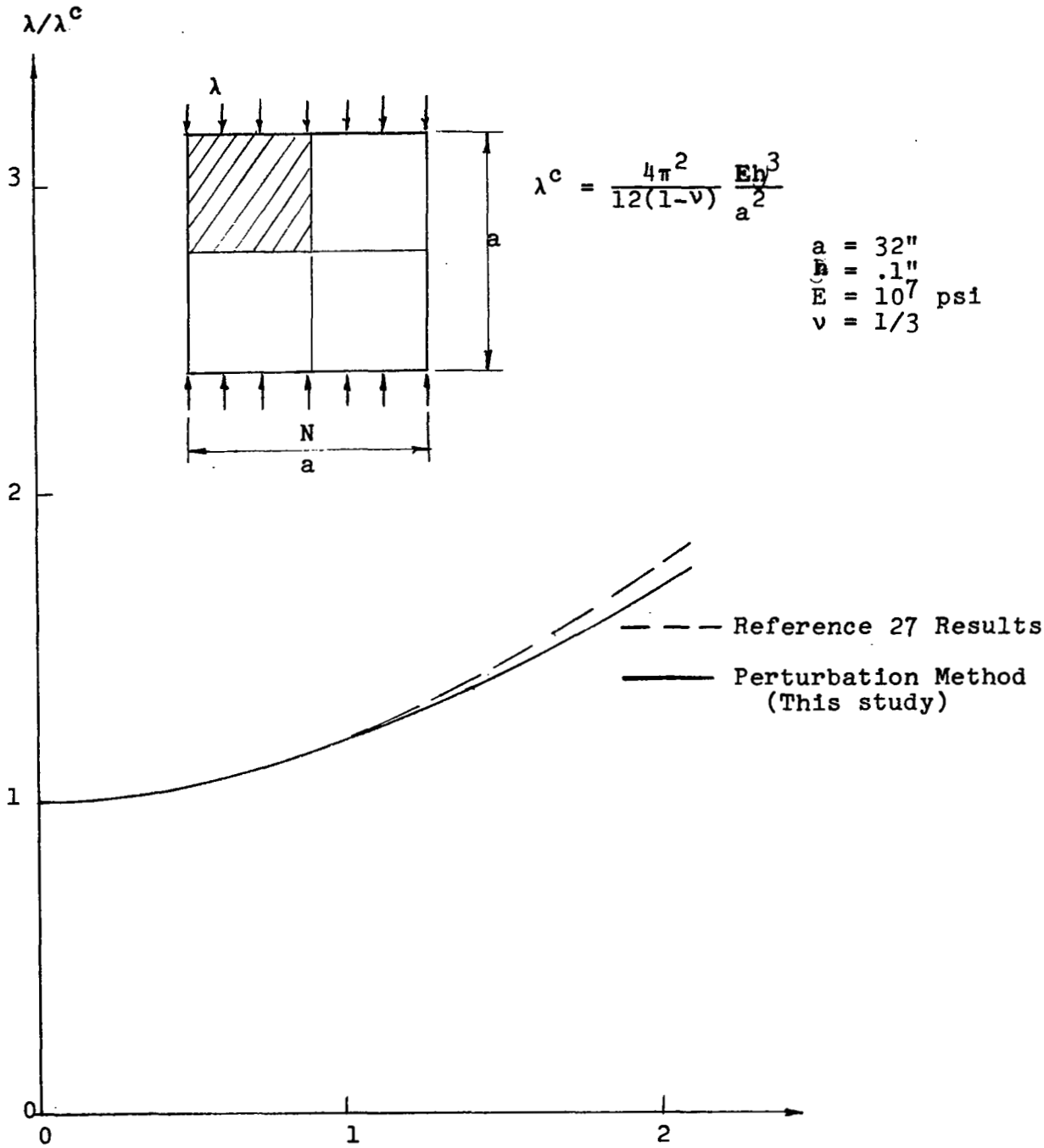

FIGURE 13. FLAT PLATE. LOAD VERSUS CENTRAL DEFLECTION.

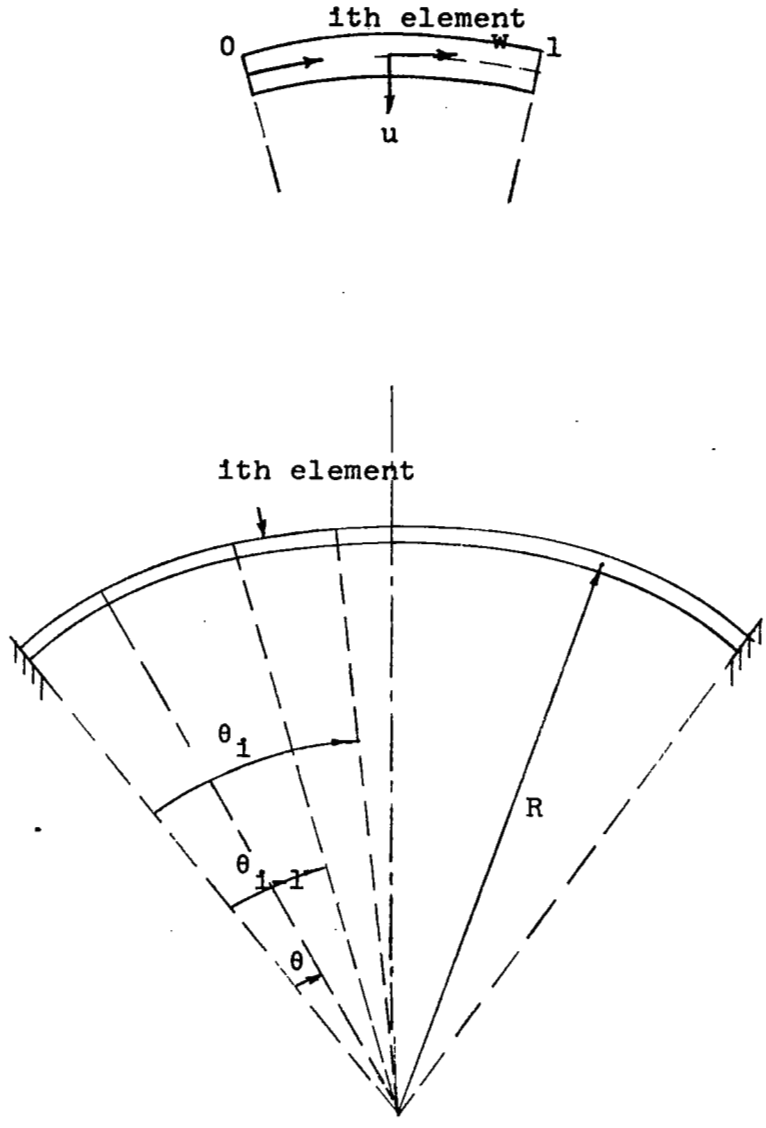

FIGURE A-1. ARCH PROBLEM. LOCAL COORDINATE

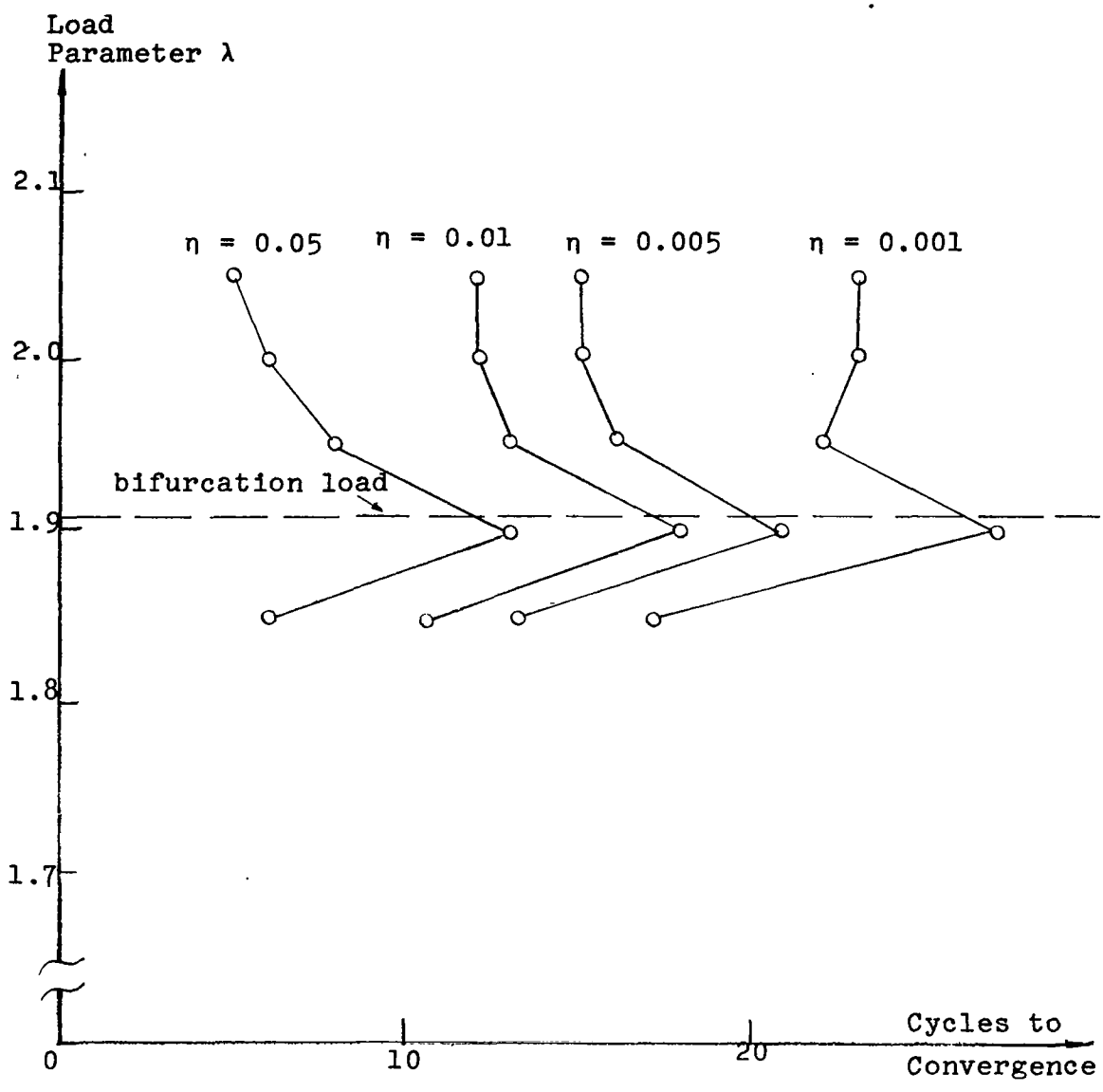

FIGURE A-2. NUMBER OF ITERATIONS FOR CONVERGENCE VS. LOAD LEVEL FOR VARIOUS CONVERGENCE CRITERIA (η)